

OPTIMIZATION OF COBALT ELECTRODEPOSITION FROM COBALT CHLORIDE
USING UREA AND CHOLINE CHLORIDE IONIC LIQUID

by

ANDREA R. KIM

RAMANA G. REDDY, COMMITTEE CHAIR
MARK WEAVER
DANIEL FONSECA

A THESIS

Submitted in partial fulfillment of the requirements
for the degree of Master of Science
in the Department of Metallurgical and Materials Engineering
in the Graduate School of
The University of Alabama

TUSCALOOSA, ALABAMA

2016

Copyright Andrea R Kim 2016

ALL RIGHTS RESERVED

ABSTRACT

The novel process for the electrodeposition of cobalt using the urea and the choline chloride ionic liquid (2:1 molar ratio) was studied to search the optimized parameters for the higher current efficiency. Scanning electron microscope (SEM) and X-ray diffraction (XRD) were used for the characterization of cobalt deposits after conducting experiments.

The cyclic voltammetry was tested with 0.2M CoCl₂ using various scan rates to determine the reduction potential in Urea/ChCl at 323K. Based on the data from cyclic voltammetry test, the transfer coefficient and the diffusion coefficient were calculated as 0.22 and $3.38 \times 10^{-6} \text{cm}^2/\text{s}$, respectively.

The electrodeposition experiment was performed with the copper sheet and the graphite sheet as a working electrode and a counter electrode, respectively. The used parameters were various temperatures (323K to 383K), applied potentials (2.4V to 3.3V), and concentration of CoCl₂ (0.2M to 0.5M). Current efficiency and energy consumption were calculated to find the optimal condition for the electrodeposition of cobalt. Variation of temperatures did not influence the current efficiency in range of 323K to 383K but the data at 323K showed the highest efficiency with the lowest energy consumption. Higher applied voltage caused the dendrite of cobalt deposition on the copper cathode, which reduced current efficiency. The CoCl₂ concentration at 0.5M maximized cobalt deposition and resulted in more than 90 % of current efficiency (95%) by increasing the diffusion rate.

SEM images showed the surface morphology of cobalt deposits on the copper cathodes according to the different parameters. As the temperature increases, the particles in the cobalt deposits grew larger without changing their shape. The higher applied voltage showed dendrites on the surface of the copper sheet at 3.3V and the measured average size of the dendrites was 156 μm . Increasing the concentration of CoCl_2 didn't show the large change of the particle size except for the thicker coverage of cobalt layer.

Elemental analysis was studied using XRD with two samples from the 6hour electrodeposition experiment. One was the cobalt powder from the cobalt dendrite deposit, which was easily detached, and the other was the thick cobalt layer on a copper cathode. They showed the pure cobalt peaks without any other elements.

DEDICATION

This thesis is dedicated to all people including my family, the lab group members and the faculty members who gave enormous help to finish my studying.

ACKNOWLEDGEMENTS

First, I would like to give my gratitude to my advisor, Professor Ramana G. Reddy for the guidance and the encouragement to finish my research successfully during my graduate studying period through his experience and knowledge. I also want to show my appreciation to Dr. Haoxing Yang, Min Li, and Mallikharjuna R. Bogala for teaching me the procedure of my research and giving me a suggestion for better results. I would like to extend my gratitude to my other research members who have supported my work.

I would like to thank Dr. Mark Weaver and Dr. Daniel Fonseca for attending on my committee in spite of their busy schedule. Their suggestion and comments are really helpful for my academic experience.

I would like to thank the Department of Metallurgical and Materials Engineering, The University of Alabama for giving me an opportunity to further my studies. I would like to acknowledge the financial support from the National Science Foundation (NSF) under the grant number NSF-No.1310072 throughout this research work.

I would like to thank my parents for giving me birth and raising me with their endless financial and emotional support. Although I had a hard time due to various reasons, they always stood beside me and encouraged me for my future. Again, I would like to give the unlimited gratitude and appreciation to my parents.

CONTENTS

ABSTRACT.....	ii
DEDICATION.....	vi
ACKNOWLEDGEMENTS.....	v
LIST OF TABLES.....	viii
LIST OF FIGURES.....	ix
CHAPTER 1. INTRODUCTION.....	1
1.1 Introduction of Cobalt and Cobalt Production.....	2
1.2 Schematic Description of Primary Cobalt Refineries.....	5
1.3 Chloride Leaching of Matte by Electrowinning.....	6
CHAPTER 2. LITERATURE REVIEW.....	8
2.1 Ionic Liquids.....	8
2.1.1 Chronological Study of Ionic Liquids.....	8
2.1.2 DES containing Choline Chloride.....	10
2.1.3 Application of ChCl/Urea DES.....	13
2.2 Electrochemical Study.....	14
2.2.1 Controlled-Potential Method.....	14
2.2.2 Cyclic Voltammetry.....	15
2.2.3 Chronoamperometry.....	17
CHAPTER 3. RESEARCH OBJECTIVES.....	20

CHAPTER 4. EXPERIMENTAL PROCEDURE.....	21
4.1 Synthesis of Ionic Liquid.....	21
4.2 Dissolving Cobalt Chloride in Ionic Liquid	22
4.3 Electrochemical Measurement Setup	23
4.3.1 Cyclic Voltammetry	24
4.3.2 Electrodeposition of Cobalt.....	25
4.3.3 SEM Analysis.....	27
4.3.4 XRD Analysis	27
CHAPTER 5. RESULTS AND DISCUSSION	29
5.1 Cyclic Voltammetry	30
5.2 Effect of Temperature on Electrodeposition of Co	32
5.3 Effect of Applied Voltage on Electrodeposition of Co	38
5.4 Effect of Concentration of CoCl ₂ on Electrodeposition of Co	44
5.5 Chemical Element Analysis of Co Deposit	50
CHAPTER 6. CONCLUSION	52
REFERENCES	54
APPENDIX I	60
APPENDIX II	64
APPENDIX III.....	69

LIST OF TABLES

Table 2.1. Molar ratio, freezing point, and various chemical and general properties of DES based on ChCl with different hydrogen bond donors at 80°C.

Table 2.2. Price of various hydrogen bond donors to synthesize DES based on ChCl.

Table 4.1. Parameters used in the CV experiments.

Table 4.2. Parameters of the electrodeposition of cobalt to search the optimum parameters.

Table 4.3. Parameters of the samples to use the elemental analysis with XRD.

Table 5.1. The transfer coefficient and the diffusion coefficient in various ionic liquid systems.

Table 5.2. Summary of the current efficiency and the energy consumption according to temperature. (Concentration of $\text{CoCl}_2 = 0.2\text{M}$, Cell volatage = 3.0 V)

Table 5.3. Summary of the current efficiency and the energy consumption according to the reduction potential. (Concentration of $\text{CoCl}_2 = 0.2\text{M}$, Temperature = 323K)

Table 5.4. Summary of the current efficiency and the energy consumption according to the concentration of CoCl_2 . (Temperature = 323K, Cell volatage = 2.7V)

LIST OF FIGURES

Figure 1.1. Application of cobalt in 2014.

Figure 1.2. World cobalt production in 1900's.

Figure 1.3. Cobalt production as a function of years (1995-2008) with different countries.

Figure 1.4. Flow chart of Falconbridge process using chlorine gas.

Figure 2.1. Phase diagram of ChCl/Urea.

Figure 2.2. Schematic cyclic voltammetry curve: (a) the basic potential sweeping program (b) the current response of the diffusion free electrochemical system (c) the current response of the electrodeposition of metals stripping.

Figure 2.3. Schematic chronoamperometry plots: (a) the potential change as a function of time, (b) the simulated concentration at different times, (c) the current response as a function of time.

Figure 2.4. (a) Typical current response with time and (b) schematic demonstration of the growth of nuclei in overlapping the hemispherical diffusion zone resulting in the linear diffusion to electrode.

Figure 4.1. Flow chart of the synthesis of ChCl/Urea (1:2 molar ratio) mixture.

Figure 4.2. Transparent homogeneous solution of ChCl/Urea (1:2 molar ratio) mixture.

Figure 4.3. ChCl/Urea (1:2 molar ratio) solution with 0.2 M of CoCl_2 .

Figure 4.4. EG&G PARC model 273A Potentiostat/Galvanostat with Power Suit software.

Figure 4.5. (a) Schematic and (b) actual CV experiment setup.

Figure 4.6. (a) Schematic and (b) actual electrodeposition setup.

Figure 4.7. Photographs of (a) the copper cathode and (b) the cobalt deposited copper cathode.

Figure 4.8. Images of (a) the Co deposits on the copper cathode and (b) the Co deposit powders stuck on a magnetic stirrer from 6 hour experiments.

Figure 5.1. Cyclic voltammogram of Urea/ChCl (2:1 ratio) with 50 mV/s scan rate at 323K.

Figure 5.2. Cyclic voltammogram of 0.2M CoCl₂-Urea/ChCl according to the various scan rates at 323K. (Inset: Cathodic current density peaks of CV of 0.2M CoCl₂-Urea/ChCl as a function of various scan rates at 323K.)

Figure 5.3. Cathodic current density peaks from cyclic voltammogram of 0.2M CoCl₂-Urea/ChCl as a function of various scan rates at 323K .

Figure 5.4. Current density as a function of time at various temperatures under the applied voltage 3.0V and concentration 0.2M of CoCl₂.

Figure 5.5. SEM micrographs of Co electrodeposits at (a) 323K, (b) 353K, (c) 363K, (d) 383K under the applied voltage 3.0V, concentration 0.2M of CoCl₂ and 2 hours.

Figure 5.6. SEM micrographs of cross-sectional Co electrodeposits at (a) 323K and (b) 383K under the applied voltage 3.0V, concentration 0.2M of CoCl₂, and 2 hours.

Figure 5.7. Current density as a function of time at the different applied voltage under the temperature 323K and concentration 0.2M of CoCl₂.

Figure 5.8. SEM micrographs of Co electrodeposits at the applied voltages (a) 2.4V, (b) 2.7V, (c) 3.0V, (d) 3.3V under the temperature 323K, concentration 0.2M of CoCl₂ and 2 hours.

Figure 5.9. SEM micrographs of cross-sectional Co electrodeposits according to the applied voltages (a) 2.4V and (b) 3.3V under the temperature 323K, concentration 0.2 M of CoCl₂ and 2 hours.

Figure 5.10. SEM micrographs of the single dendrite of Co electrodeposits under the temperature 323K, concentration 0.2M of CoCl₂, the applied voltage 3.3V, and 2 hours.

Figure 5.11. Current density as a function of time at the different concentrations of CoCl₂ under the applied voltage 2.7 V and temperature 323K.

Figure 5.12. SEM micrographs of Co electrodeposits according to the concentration of CoCl_2 (a) 0.2M, (b) 0.3M, (c) 0.5M under the applied voltage 2.7 V, the temperature 323K and 2 hours.

Figure 5.13. SEM micrographs of the cross-sectional Co electrodeposits according to the concentration of CoCl_2 (a) 0.3M and (b) 0.5M under the applied voltage 2.7V, temperature 323K and 2 hours.

Figure 5.14. Saturated 0.6 M CoCl_2 -Urea/ChCl solution.

Figure 5.15. XRD pattern of the Co electrodeposits for 6 hours under the concentration 0.5M of CoCl_2 at (a) the applied voltage 3.3V and temperature 363K and (b) applied voltage 2.7V and temperature 323K.

CHAPTER 1

INTRODUCTION

Humans discovered metals in 8000 B.C and have developed the extraction process of metals till present time. Since metals have been required for various purposes such as the construction, the engineering application, and the weapon industry as time goes by, the metallurgy and the metal extraction in production in a large scale became more important especially after the industrial revolution. Metals generally exist as oxides, sulfides, and oxysalts form in the earth's crust. The metal extraction process is governed by its physical and chemical properties with the availability of ores. In general, the mining process consists of:

- i. Comminution: decreasing a size of particle for splitting the valuable metals from the useless parts.
- ii. Separation: separating materials with different chemical properties and physical properties for many advantages in future application.

The metal extractions in commonly use can be described as:

- 1) Pyrometallurgy: Metal extraction process using heat and a reducing agent at high temperature. The reaction takes place of metal reductions from other undesired matters with gas or slag form.

- 2) Electrometallurgy: The process of refining or purifying metals using electricity. The electrometallurgy can be referred as electrowinning, electrorefining, electroplating, and electroforming. Each process has a different purpose. Electrowinning is the extraction metals from ores using the electrode cells and electrolyte, electrorefining is used for the purification of metals, electroplating is depositing a layer of a metal on other metal, and electroforming is synthesizing a thin layer of metal.
- 3) Hydrometallurgy: Metal extraction technique using aqueous solution with ores, concentrates, and recycles materials [1]. This method is governed by the three processes; leaching, solution concentration and purification, and metal recovery. Leaching is simply the extraction of minerals from ore using aqueous liquid. Solution concentration and purification is recovering the concentration of the metal ion in leaching solution after leaching and removing unwanted metal ions. Metal recovery is the last process of hydrometallurgy producing high grade metals. The metal recovery includes electrolysis, gaseous reduction, and precipitation.

1.1 Introduction of Cobalt and Cobalt Production

Cobalt is the 33rd abundant element (0.0025%, 20ppm) on the earth's crust. It usually has a formation of arsenides, sulfides, and oxide with other element such as nickel and copper. Thus, cobalt is generally produced as a by-product of other metal extraction in general. Since cobalt has silver-grey glossy appearance with unique properties, it has been used in many applications. Cobalt applications of cobalt have been found in Egyptian pottery and Iranian glass beads as a blue color earlier than 2200 BC. Swedish chemist Georg Brandt succeeded to isolate the cobalt metal in 1735 and Torbem Bergman enhanced it subsequently in 1780 [2].

After World War II, the demand for the high purity of cobalt metal increased significantly due to the requirement for aircraft jet engines and gas turbines. As shown in Figure 1.1, applications of cobalt in recent days are varied by different purposes. Most usages of cobalt are the batteries for a cathode in Li-ion battery for mobile phones and laptops [3]. Furthermore, increasing of hybrid vehicles causes more demand of rechargeable batteries contained cobalt. Super alloys with cobalt are really important, which has corrosion resistance and endures high elevating temperature. They are mainly used in aerospace industry, where higher operating temperature enhances the high efficiency of engine fuel. Obviously, the super alloys containing cobalt are still being used in military and commercial jet engines and turban blades as well [4]. Cobalt based alloys are also used in magnets and biomedical technologies for orthopedic implants and prosthetics [5-7]. Demand of cobalt is increasing due to various applications in many fields. As the demand of cobalt metals increases, the demand of other major metal such as nickel was also increased for use in stainless steel to build nuclear reactors [8].

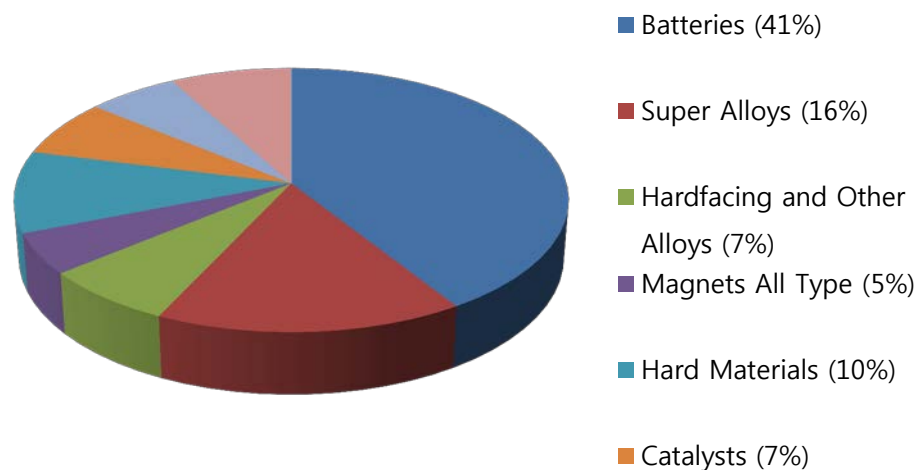


Figure 1.1. Application of cobalt in 2014 [3].

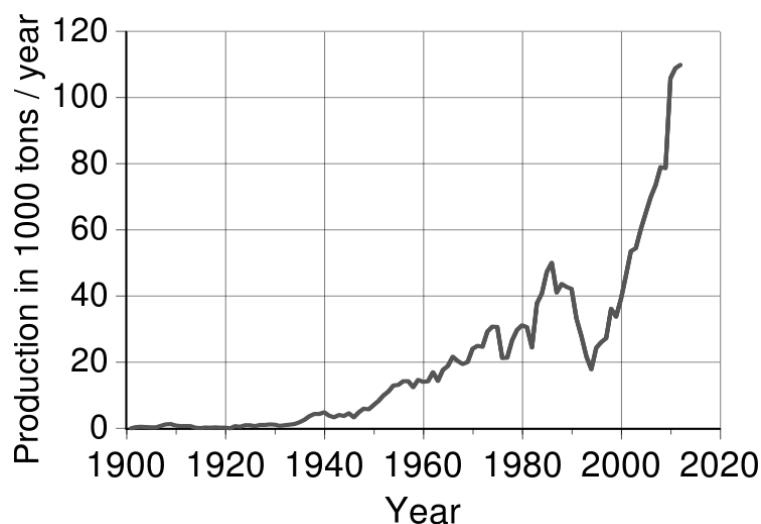


Figure 1.2. World cobalt production in 1900's [9].

In the early 19th century, cobalt deposits were founded in many countries in Europe and South America continents. The oxidized cobalt mines were developed in New Caledonia and became a major cobalt source in the late 19th century. In 1904 silver-cobalt-arsenic ores were discovered in Ontario, Canada where turn into the major cobalt source after New Caledonia. Cobalt Arsenide ores were founded in Bou-Azzer, Morocco in 1932 and Idaho, USA in 1952. The cobalt production with by-product method was invented from copper mines of Democratic Republic of Congo (DRC) in 1926 and Zambia in 1934. The first commercial cobalt electrowinning plants were constructed at Shituru, DRC in 1945 and Rhokana, Zambia in 1952 subsequently. After 1950's DRC dominated the cobalt production but decreased the source considerably after 1986. However, nickel producers which emerged cobalt (sulphides and laterites) increased, so cobalt production increased as well. According to Cobalt Development Institute, approximately 50% of cobalt was produced from nickel industry as by-product [8].

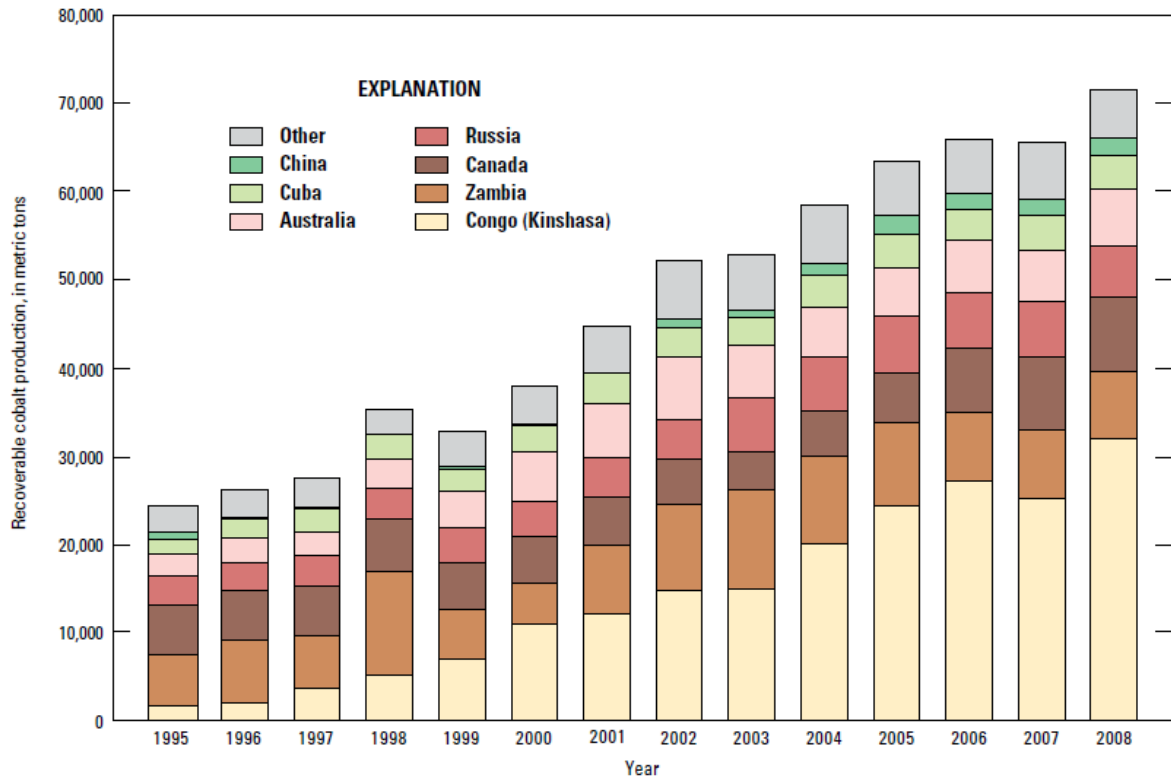


Figure 1.3. Cobalt production as a function of years (1995-2008) with different countries [10].

1.2 Schematic Description of Primary Cobalt Refineries

There are several methods to produce cobalt metal depending on compounds with cobalt:

- a. Cobalt Arsenides: This process was operated during 20th century with a roasting stage and pressure leach. However, this process was not used anymore these days due to environmental issues.
- b. Copper-Cobalt Ores: Roast-Leach-Electrowin process is the common way to recover from copper flotation concentrates. After roasting the sulphides, sulphuric acid atmospheric leach and direct electrowinning for copper are used. In recent years,

direct electrowinning process is replaced by solvent extraction and electrowinning method for better grade copper.

c. Nickel Sulphides: It is processed by flotation with smelting to produce a nickel matte which contains nickel, copper, PGMs (platinum-group metals) and cobalt. Many refineries used hydrometallurgical processes such as ammonia leach, pressure oxidation leach, sulphate oxidative leach, chlorine leach, and electro-refining due to environmental issue. Due to the environmental problem smelting steps are changing into the entire hydrometallurgical processes nowadays.

d. Nickel Oxides: Nickel laterites (oxides) are the major source of nickel as the nickel sulphides supply has been lowered from 2012. In old days, pyrometallurgical processes were used in general but were converted to hydrometallurgical method due to the environmental issue and the advantage to refine cobalt.

1.3 Chloride Leaching of Matte by Electrowinning

This process is also called “Falconbridge Process” which matte from the milled ore or concentrate is leached in chloride solution in multiple times at a high temperature and pressure as the first step. The chlorine gas is applied in the electrowinning system and flows back to the leaching circuit. Copper is precipitated as the sulphide and other residues including iron and arsenic are precipitated as hydroxides and arsenates which are used to purify leachate [11]. After copper sulphide is fed into the fluidized bed furnace for roasting and calcination, the result calcine is leached in electrolyte with spent copper. Copper metal is produced after electrowinning. Cobalt and nickel are extracted after removing copper in the matte using the chlorine solution and iron through the tailing. Cobalt is removed by the solvent extraction of the chloride solution using organic solvent and electrowon. Nickel

solution is subsequently purified the impurities such as lead and manganese using chlorine and electrowon with dimensionally stable anode and diaphragm bag in order to collect chlorine gas.

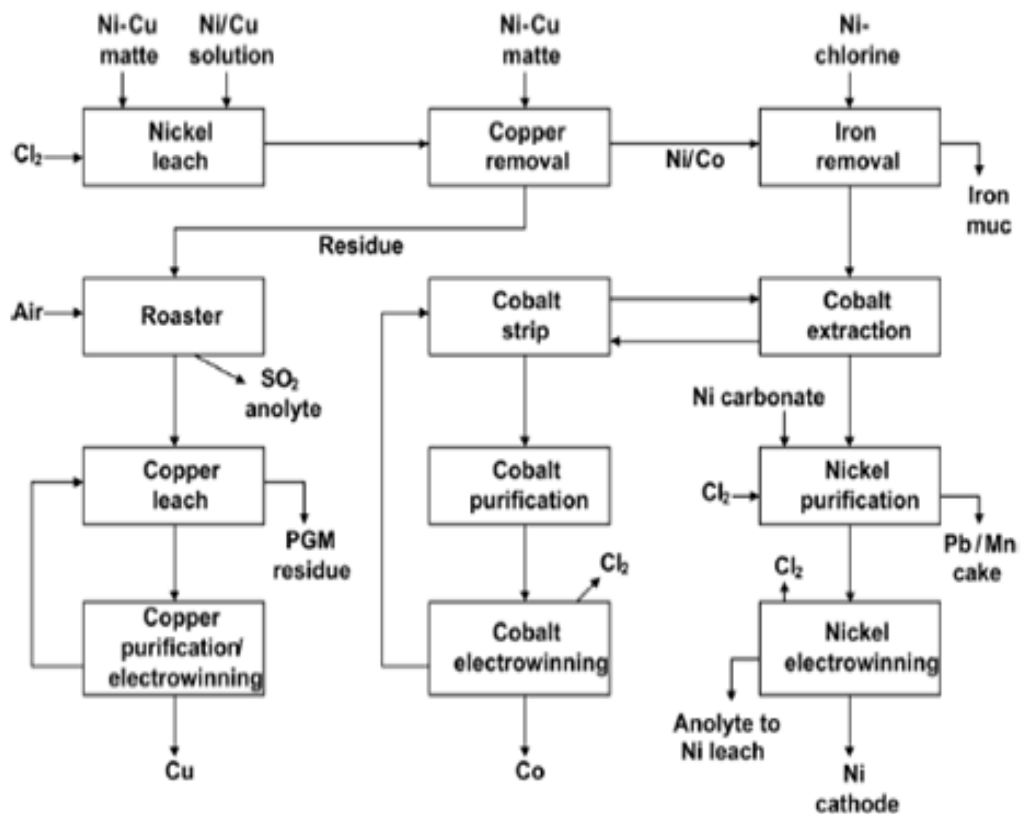


Figure 1.4. Flow chart of Falconbridge process using chlorine gas [11].

CHAPTER 2

LITERATURE REVIEW

2.1 Ionic Liquids

Ionic liquids can be easily defined by the liquid salts which the melting point is below 100°C [12-13]. Since they are formed with mostly ions, they have the over wide-chemical window. Also, they are stable as a liquid form in various temperature ranges. As an electrolyte, ionic liquids have several advantages compared to other type of solutions such as high temperature molten salts [14-17]:

- wide potential windows
- high solubility of metal salts
- high conductivity
- thermal stability
- non-flammability
- low vapor pressure

2.1.1 Chronological Study of Ionic Liquids

The first ionic liquid was [EtNH₃-NO₃] originated in 1914 by Paul Walden as a battery electrolyte [18]. Later, lots of researchers studied the ionic liquid for aluminum electrodeposition application using AlCl₃ [19-23]. Wilkes et al. created the phase diagram of [C₂mim]Cl-AlCl₃ system and figured out the stable formation with low viscosity in

AlCl_3 molar ratio from 0.33 to 0.67 at room temperature [24-25]. However, the limit of the first generation ionic liquid was revealed through many studies over many years. It was only able to prepare easily under dry surrounding due to the hygroscopic property. Therefore, the second generation ionic liquids which are more stable under air atmosphere at room temperature were invented to overcome the limits of the first generation ionic liquids. The first discovery of the second generation ionic liquid was 1-ethyl-3-methylimidazolium (C_2mim) cation with wide selections of anions such as $[\text{CH}_3\text{CO}_2]$, $[\text{NO}_3]$, $[\text{PF}_6]$, and $[\text{BF}_4]$ invented by Wilkes and Zaworotko in 1992 [26]. However, some of the second generation ionic liquid such as tetrafluoroborate (BF_4) and hexafluorophosphate (PF_6) can cause HF gas by exposure in moisture from air for long time although they have 4 volts of electrochemical window. Thus, Gratzel et al. invented the hydrophobic anions such as $[\text{TfO}]^-$, $[\text{Tf}_2\text{N}]^-$, and $[\text{Tf}_3\text{C}]^-$ ionic liquids [29-28]. Abbott et al. created a new type of ionic liquid called deep eutectic solvent (DES) which is quaternary ammonium salts such as hydroxyethyltrimethylammonium (choline) with four types of ligand agents in 2001. The four types of ligand agents are:

- Anhydrous Metal Salts (MCl_x , $\text{M}=\text{Zn}, \text{Sn}, \text{Fe}$) [29-30]
- Hydrated Metal Salts ($\text{MCl}_x \cdot y\text{H}_2\text{O}$) [31]
- Hydrogen Bond Donors (CONH_2 , COOH , OH) [32-33]
- $\text{MCl}_x \cdot \text{Z}$ ($\text{Z}=\text{urea}, \text{ethylene glycol}, \text{acetamide}$) [34]

Compared to the traditional ionic liquids, DES has additional advantages such as low price, environmental compatibility, easy storage, and easy preparation [35-36].

2.1.2 DES containing Choline Chloride

Choline Chloride is the one of quaternary ammonium salts at room temperature and can be synthesized by mixing with hydrogen bond donors at eutectic temperature. Because of its environmental and economic advantages, it has been used in various purposes such as an additive in chicken feed and synthesis of chemical compounds for choline hydroxide and choline bitartrate. As seen in Table 2.1 [37], ChCl/Urea and ChCl/Ethylene glycol have the eutectic points at molar ratio 1:2 while other systems reach to freezing point at 1:1 molar ratio. All DES systems have a similar density which is closed to water (1.00 g/cm^3). While the DES systems with oxalic acid and ethylene glycol have relatively greater electrical conductivity than ones with urea and malonic acid, viscosities of the systems with urea and malonic acid are higher than others. They all have advantage for easy availability but ChCl/Oxalic acid and ChCl/Ethylene glycol are toxic, which is not expected for environmental compatibility. Table 2.2 shows the commercial price of hydrogen bonding donors to synthesize DES with ChCl. Considering same weight of each chemical, urea and ethylene glycol have a lower price than malonic acid and oxalic acid. For the wide usage of DES as an electrolyte, low cost, high conductivity and non-toxicity are required. ChCl/Oxalic Acid and ChCl/ Ethylene Glycol are not feasible for the electrolyte due to their toxicity. ChCl/Malonic Acid is more expensive than other candidates listed in tables above, so it is not desired for the application in large scale. Therefore, ChCl/Urea would be the most appropriate substance for an electrochemical application.

Table 2.1. Molar ratio, freezing point, and various chemical and general properties of DES based on ChCl with different hydrogen bond donors at 80°C [37].

ChCl/ HBD	Molar Ratio	Freezing Point (°C)	Density (g/cm ³)	Electrical Conductivity (mS/cm)	Viscosity (cPa•s)	Availability	Toxicity
Urea	1:2	12	1.17	6.14	33.57	Easy	No
Malonic Acid	1:1	10	1.50	2.21	69.07	Easy	No
Oxalic Acid	1:1	34	1.13	12.81	13.80	Easy	Yes
Ethylene Glycol	1:2	-66	1.03	15.17	9.14	Easy	Yes

Table 2.2. Price of various hydrogen bond donors to synthesize DES based on ChCl.

HBD	Price (\$, Alfa Aesar [®] in 2016)
Urea (99.3+%)	36.18/500g
Malonic Acid (99%)	91.50/500g
Oxalic Acid (Anhydrous, 98%)	36.54/250g
Ethylene Glycol (99%)	23.95/500g

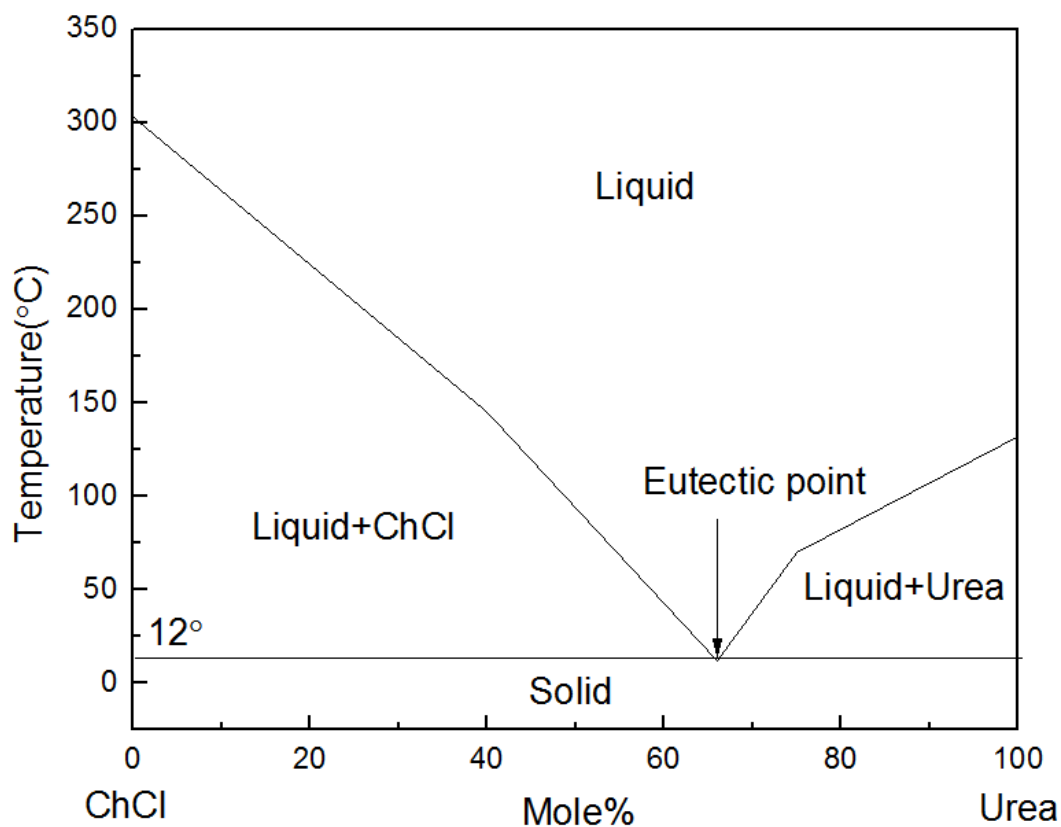


Figure 2.1. Phase diagram of ChCl/Urea.

2.1.3 Application of ChCl/Urea DES

People have applied reline (commercial name of mixture of Urea/ChCl) for the extraction and the electrodeposition of metal for several years because of lots of advantages [38]. Yang et al. investigated the solubility of ZnO in the eutectic mixture of Urea/ChCl with the FTIR spectroscopy, the cycle voltammetry, the calculations of the current efficiency and the energy consumption in various temperatures, the applied voltages, and the addition of HSO_4 for the electrodeposition of Zn with ZnO [39-40]. They also studied the solubility of PbO in reline with the same method (FTIR spectroscopy) and successfully synthesized the

pure lead on the copper substrate [41]. Cojocaru et al. [42] studied the electrochemical impedance spectroscopy of selenium behavior to present the cathodic process from the electrodeposition of Se films in reline. They reported that electrochemical impedance measurements showed that the cathodic process of selenium ions in ChCl-urea and ChCl-EG ionic liquids had almost similar characteristics. Ana-Maria et al. [43-44] discussed the electrochemical reaction in the electrodeposition of copper using reline and CuCl. Their group calculated the diffusion coefficient in CuCl and reline system. Also they studied the electrochemical behavior of CuCl₂ in reline using the cyclic voltammetry and the electrochemical impedance spectroscopy. Ali et al. [45] published the electrodeposition of copper from reline with CuCl₂. They successfully synthesized and investigated the dense, smooth, and continuous copper deposition using scanning electron microscopy and X-ray diffraction. The current efficiency of their deposition of pure copper is about 97%. Chu et al. [46] proved to form zinc-cobalt alloys from choline chloride and urea solvent mixture. They investigated that the size of grain cluster of Zn-Co deposition increases as the negative value of potential increases. Abbott group [47] deposited zinc-tin alloy in reline on the platinum electrode. Their group showed that zinc and tin could be deposited as individual metals and as an alloy. Gómez et al. [48] were successful in electrodepositing platinum on the vitreous carbon electrode. They discussed that the deposition condition depended on the nature of solvent and the deposited species because the electrochemical window had more or less wideness, factor to improve the current efficiency and minimize the damage of the coating. Costovici et al. [49] electrochemically synthesized the ZnO nano powder with the platinum cathode and zinc anode with at least 85% efficiency at 20°C~30°C. Their cyclic voltammogram showed that the continuous increasing current caused the dissolution of Zn and the oxidation of O₂²⁻ at the same time to synthesize the precipitated ZnO in the anodic

scan. Anicai et al. [50] studied the electrodeposition of Ni on Cu substrate with some cracks due to the corrosion behavior on it. They also performed the cyclic voltammetry to investigate that the limit cathodic peaks for Ni (II) reduction at 30°C and 80°C were located at -1.05V and -0.75V to -0.88V, respectively. Huynh et al. [51] used choline chloride/ urea (1:1 molar ratio) to synthesize Al from AlCl₃ on glassy carbon, iron, and copper cathodes, whose current efficiencies were 30.8%, 64.45%, and 29%, respectively. They also analyzed the purities of Al depositions on each cathode, which were 92.42% for glass carbon, 70.33 % for iron, and 82.63% for copper, respectively. Golgovici et al. [52] performed the electrodeposition of Cd and CdTe on the platinum cathode from TeO₂ and CdCl₂. They observed only one couple of reduction/oxidation peaks from Cd²⁺ ion and the complex shape due to Cd²⁺ /Te⁴⁺ ions using the cyclic voltammetry. Li et al. [53] reported the electrodeposition of Co from CoCl₂ on copper cathode. They used the cyclic voltammetry to study that two irreversible reactions occurred from Co(II) to Co with one-step two electron process. They also calculated the diffusion coefficient at 373K, the current efficiency at various temperatures, and the reduction potentials.

2.2 Electrochemical Study

2.2.1 Controlled-Potential Method

Electrochemical study is important for the electrodeposition of metal because it is used to study not only the characterization of the ionic liquids, but also the electrode behavior in the electrolyte. Thus, the electrochemical active species as a function of the applied potential are able to determine the current response of oxidation or reduction reaction of the electrode through the controlled-potential method. Current response can be explained by the rate of mass transfer and the rate of electron transfer between electrode and solution interface.

The mass transfer is able to describe into three forms: (a) migration, (2) diffusion, and (3) convection. The Nernst-Planck equation [54] is used to explain the relationship of the mass transfer and the three forms in one dimension, x :

$$J(x, t) = -\frac{nFDC_0^*}{RT} \frac{\delta\varphi(x, t)}{\delta x} - D \frac{\delta C(x, t)}{\delta x} + C^* v(x, t) \quad (2.1)$$

where $J(x, t)$ is the flux of active species at x in m distance from the electrode surface, D is the diffusion coefficient, C^* is the concentration of species, $\frac{\delta\varphi(x, t)}{\delta x}$ is the potential gradient, $\frac{\delta C(x, t)}{\delta x}$ is the concentration gradient, and $v(x, t)$ is the convection component. The electromigration can be neglected performing the controlled-potential experiment because ionic liquids are ionic solvent which are unnecessary to add the inert electrolyte (supporting electrolyte). The function of convection from the vibrations and the non-equal heating of solution is not preferred in this work. It can be minimized by the stirring rate in the system. On the other hand, the mass transfer to investigate the controlled-potential method can be controlled by the diffusion of electro-active species in contact to the electrode surface.

2.2.2 Cyclic Voltammetry

Cyclic Voltammetry is an electrochemical measurement by sweeping the potential of the planar working electrode immersed in the stable system (solution). As shown in Figure 2.2, E_i is the initial potential applied to the working electrode and E_λ is the switching potential which is changing linearly. When the electro-active species are electrolyzed, the initial potential changes with a constant rate (scan rate) in mV/s. This process is known as the linear sweep and the linearly changing potential becomes to the switching potential. After the

potential reaches E_λ , the scanning direction changes into the opposite way and then the potential goes back to E_i . The electrochemical window of the ionic liquid which is able to observe the electrochemical reaction varies the potential range between E_i and E_λ . Figure 2.2b represents that the current change at the forward and the backward sweep shows the symmetry as a function of the potential in general. However, the cyclic voltammetry curve can be unlike Figure 2.2b depending on the electrodeposition of different metal, as shown in Figure 2.2c.

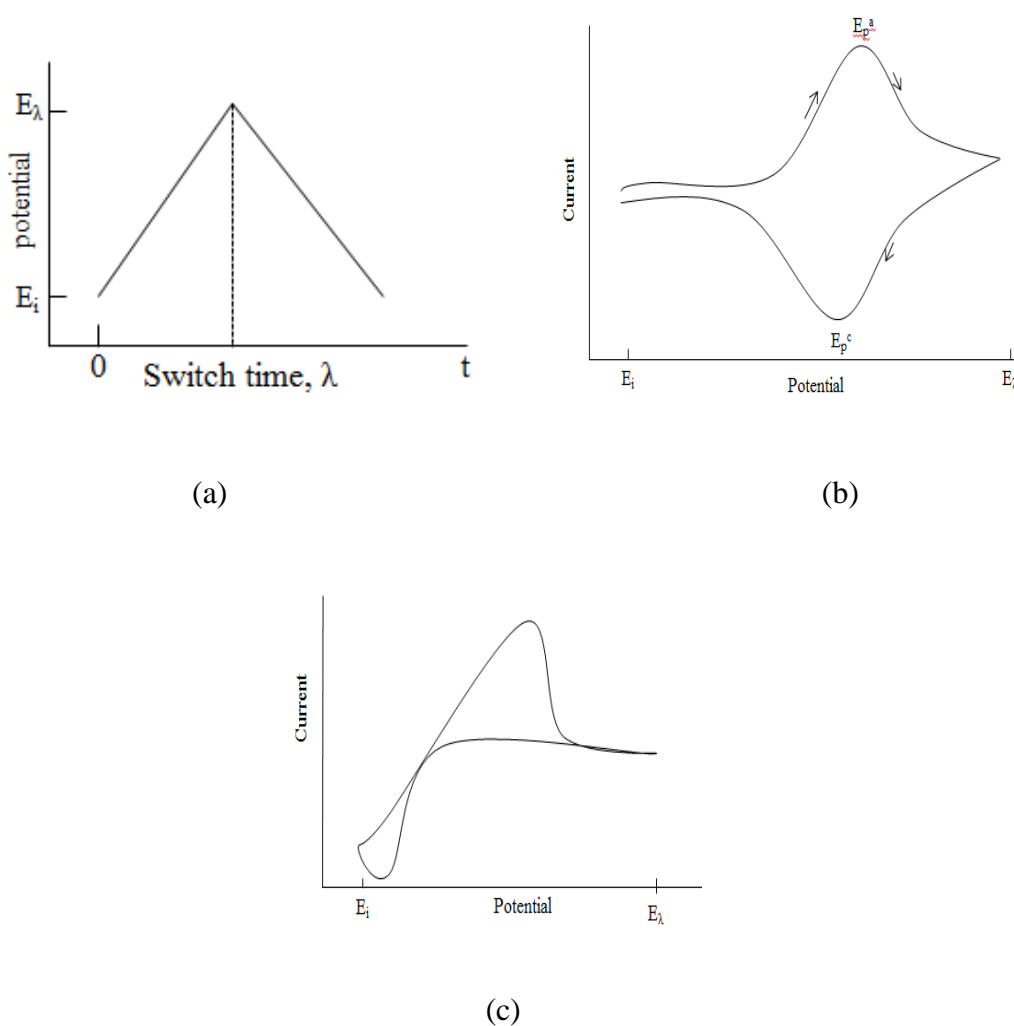


Figure 2.2. Schematic cyclic voltammetry curve: (a) the basic potential sweeping program (b) the current response of the diffusion free electrochemical system (c) the current response of the electrodeposition of metals stripping

2.2.3 Chronoamperometry

Chronoamperometry is a method to study the electrochemical characterizations of ionic liquids and the electrode reactions in the electrolyte. It is based on the diffusion of electrochemically active species with the concentration gradient $\frac{\delta C(x,t)}{\delta x}$ in equation (2.1) to the electrode surface in the migration-free and the convection-free bulk solution. It starts with the starting potential (E_1) which does not include Faradaic process to more negative potential. As the potential moves to certain negative direction with the oxidation and reduction reaction, it reaches the mass transfer-limit region (E_2). The metal ion (M^{n+}) is converted to the metal element (M) with the current during this process on the electrode surface. In the initial stage, the concentration gradient $\frac{\delta C(x,t)}{\delta x}$ is large but diffusion layer thickness δx is small. While the diffusion layer thickness δx increases, the concentration gradient decreases as the time increases in the reduction metal process to the working electrode. The following equation demonstrates a relationship of current responses and the concentration gradient $\frac{\delta C(x,t)}{\delta x}$.

$$i = nFAD \frac{\delta C(x,t)}{\delta x} \quad (2.2)$$

Figure 2.3 shows the typical graphic profiles for the potential, the concentration, and the current as a function of time which can describe the chronoamperometry mechanism [55].

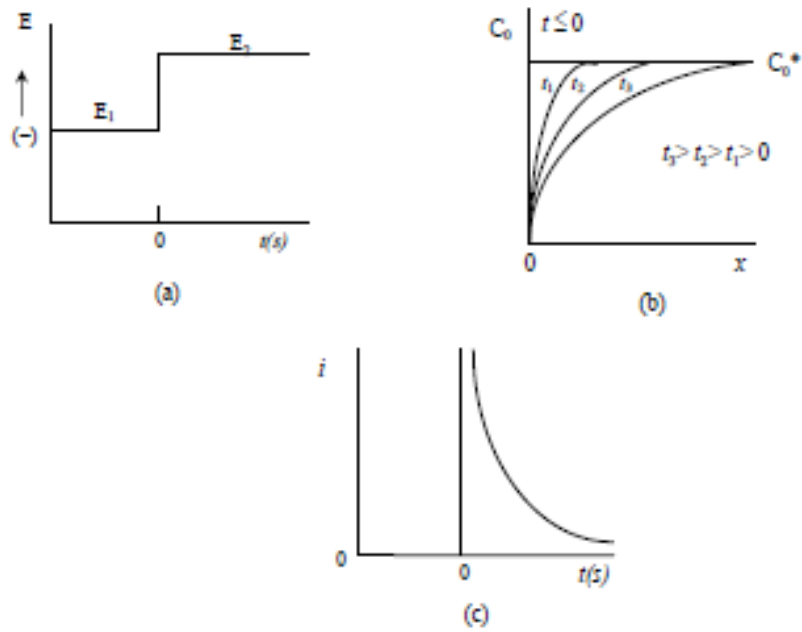


Figure 2.3. Schematic chronoamperometry plots[55]: (a) the potential change as a function of time, (b) the simulated concentration at different times, (c) the current response as a function of time.

The current is linearly proportional to the concentration gradient from equation (2.2). The current response for the linear diffusion to a planar disk electrode with time can be calculated using Cottrell equation [52]:

$$I = nFAC\left(\frac{D}{\pi}\right)^{1/2}t^{-1/2} \quad (2.3)$$

where I is the current, A is the surface area of the electrode, D is the diffusion coefficient, C is the bulk concentration, n is the number of exchange electrons, and t is the time.

The growth process of nuclei in the electrodeposition of metals occurs in the deviation from Cottrell behavior of the linear diffusion of M^{n+} to the entire electrode surface area. Figure 2.4a represents a typical current response as a function of time for a potential step

while the overpotential is applied to nucleation process. A small current flow is detected right after applying a potential pulse because of the double layer charging. The current increases as a result of the growth process of nuclei with metal deposit. Diffusion results in the growth of crystals in the multiple hemispherical fields in the nucleation stage. Finally, the charging current reaches its limit (i_m) at t_m due to coalescence of growing crystals in the individual diffusion zones. The magnitude of i_m depends on the overpotential. After the current reaches i_m , the increment of current stops and begins to decrease with typical $t^{-1/2}$ decay, which is expected for the linear diffusion to a planar surface as explained in Cottrell equation. Figure 2.4b schematically demonstrates the nucleation process and the change in the diffusion from hemispherical to planar due to the overlapping of the hemispherical diffusion zone.

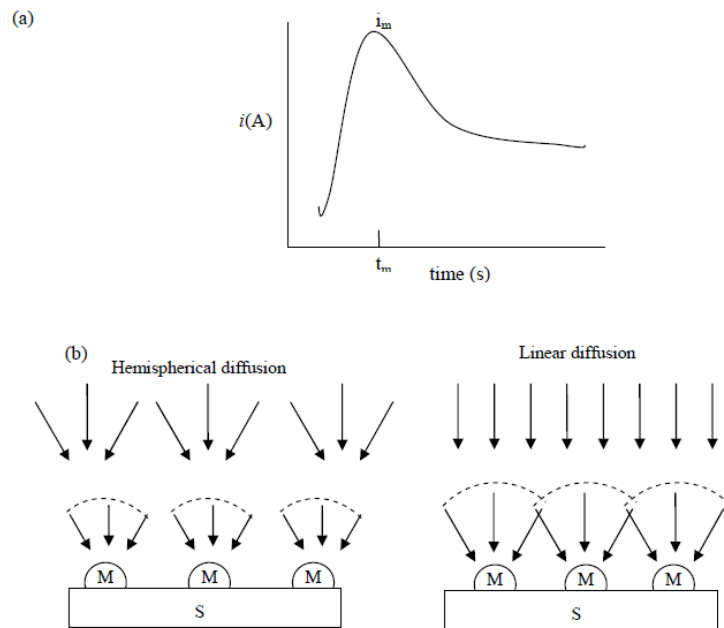


Figure 2.4. (a) Typical current response with time and (b) schematic demonstration of the growth of nuclei due to the overlapping of the hemispherical diffusion zone resulting in the linear diffusion to electrode.

CHAPTER 3

RESEARCH OBJECTIVES

The main goal of the research is to extract cobalt metals from cobalt chloride using urea and choline chloride ionic liquid. Sulfuric acid has been used as an electrolyte in industrial metal extraction process in general. However, this process has some disadvantages such as environmental issues which include emitting CO, CO₂ or SO₂ gases and high current maintenance. The objectives of the research are to study the electrodeposition of cobalt which produces less harmful gases with a less energy consumption. Thus, the research is focused on investigating the experimental parameters which lead the optimized consequences with high current efficiency. The following lists encompass the main objectives of this research:

- A. To synthesize Urea/ChCl ionic liquid with molar ratio 2:1 at low temperatures
- B. To dissolve cobalt chloride in various temperatures with different concentrations in Urea/ChCl eutectic mixture
- C. To study the experimental parameters such as temperature, applied voltage, and concentration of cobalt chloride for the high current efficiency
- D. To calculate the transfer coefficient and the diffusion coefficient which influence the metal reduction
- E. To characterize the cobalt deposits on the cathode
- F. To study the energy calculation in the electrolytic process of Co

CHAPTER 4

EXPERIMENTAL PROCEDURE

4.1 Synthesis of the Ionic Liquid

The ionic liquid (ChCl/Urea, 1:2 molar ratio) was synthesized in the laboratory as the method written in the literatures [39]. Choline Chloride ($C_5H_{14}ClNO$, 98%) and urea ($CO(NH_2)_2$, 99.3%) were used in Alfa Aesar[®]. First, they were dried for more than 2 hours to remove residual moisture in the salts. Then, they were mixed with correct molar ratio in a Pyrex beaker from Fisher Scientific Company. The two mixed salts in the beaker were heated at 363K until they formed a transparent homogeneous solution for more than 12 hours, as shown in Figure 4.2.

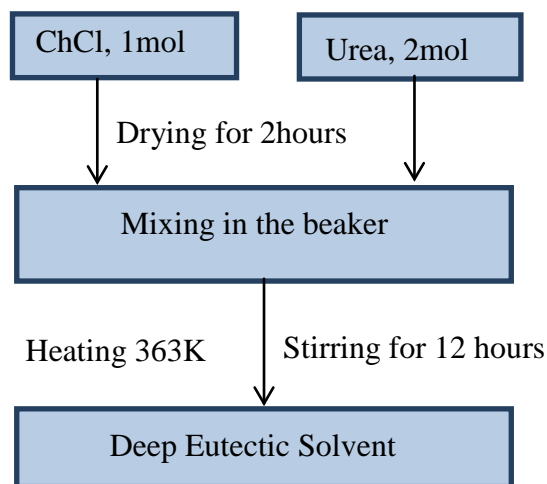


Figure 4.1. Flow chart of the synthesis of ChCl/Urea (1:2 molar ratio) mixture.

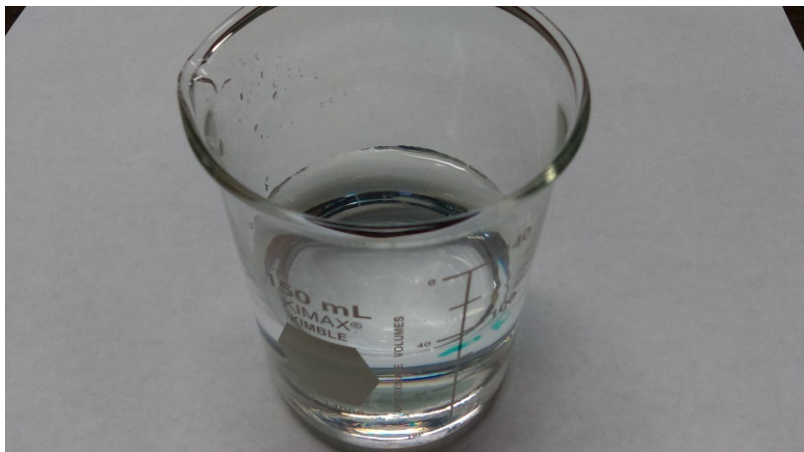


Figure 4.2. Transparent homogeneous solution of ChCl/Urea (1:2 molar ratio) mixture.

4.2 Dissolving Cobalt Chloride in the Ionic Liquid

Anhydrous cobalt chloride (II) salts (99.7%) were purchased from Alfa Aesar[®] for electrodeposition experiments with different parameters. Cobalt chloride salts for the desired concentration as molar ratio were calculated, weigh, and dissolved into the ChCl/Urea (1:2 molar ratio) ionic liquid at 363K. They were dissolved longer than 12 hours to confirm the homogenous solution without saturation. The dissolved solution formed a dark blue color. Total 0.2M, 0.3M, and 0.5M concentrations of ChCl/Urea-CoCl₂ electrolyte were used for performing experiments.

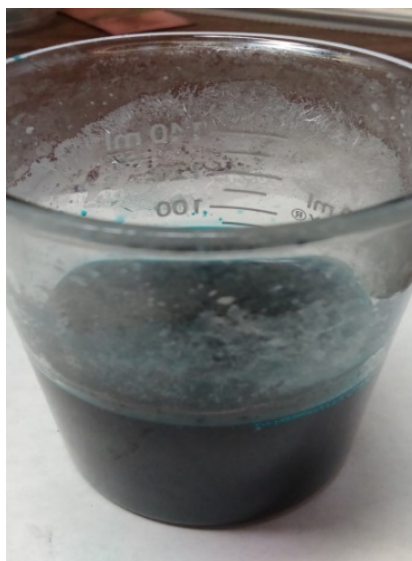


Figure 4.3. ChCl/Urea (1:2 molar ratio) solution with 0.2M of CoCl_2 .

4.3 Electrochemical Measurement Setup

EG&G PARC model 273A Potentiostat/Galvanostat and Power Suit software from Princeton Applied Research [56-59] to control the equipment were used for the cyclic voltammetry and the electrodeposition experiments using the chronoamperometry.



Figure 4.4. EG&G PARC model 273A Potentiostat/Galvanostat with Power Suit software.

4.3.1 Cyclic Voltammetry

Tungsten wire, silver wire, and platinum wire were used as a working electrode, a reference electrode, and a counter electrode, respectively. All electrodes were cleaned by SiC papers until it is shiny to obtain better results by eliminating oxides on the surface and washed with the deionized water. The electrodes were fixed in a rubber cap with a thermometer and were covered on a beaker filled in ChCl/Urea mixture (1:2 molar ratio). The CV test was performed using the pure reline and the reline with 0.2M CoCl_2 at 323K using a heating plate. The scan rate range used was 20mV/s to 80mV/s to determine the reduction potential of the reline with 0.2M CoCl_2 at 323K. The detail experiment parameters are listed in Table 4.1.

Table 4.1. Parameters used in the CV experiments.

Parameters	Values
Working Electrode	W (0.483mm)
Reference Electrode	Ag (1.27mm)
Counter Electrode	Pt (0.102mm)
Concentration of CoCl_2	0.2M
Temperature	323K
Scan Rate	20-80mV/s
Electrodes Distance	1cm

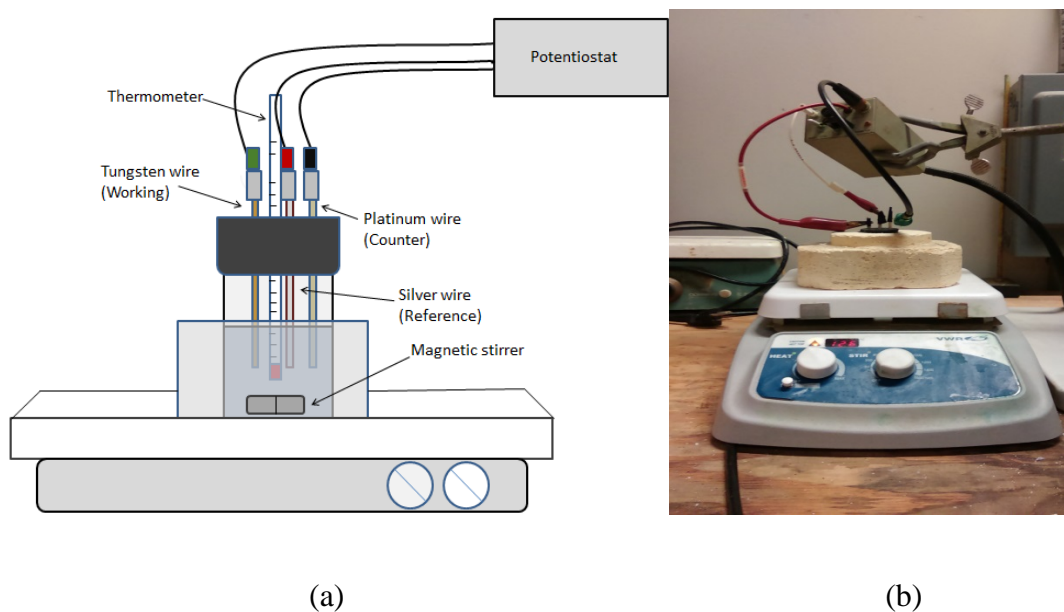


Figure 4.5. (a) Schematic and (b) actual CV experiment setup.

4.3.2 Electrodeposition of Cobalt

The copper sheet was the working electrode and the graphite sheet was the counter electrode. Both working and counter electrodes were cut to appropriate size ($2.5\text{cm} \times 5\text{cm}$) to fit into the beaker. The copper sheet was polished by SiC papers with the same reason in the CV test. The electrodes were fixed in Teflon plate using the bolts and the nuts. The insulator is shaped to fit into the beaker. The experiment of electrodeposition of cobalt from the cobalt solutions with the urea and the choline chloride had been performed for 2 hours with variation of temperatures, cell voltages, and concentrations of CoCl_2 . The temperature variation range was from 323K to 383K, the applied voltage range was from 2.4V to 3.3V, and the concentration of CoCl_2 range was from 0.2M to 0.5M, as shown in Table 4.2. The

deposited cobalt on cathode was rinsed with the deionized water and the ethanol, and then dried to analyze using SEM and XRD.

Table 4.2. Parameters of the electrodeposition of cobalt to search the optimum parameters

Parameters	Values
Working Electrode	Cu (2cm × 2.5cm)
Counter Electrode	C (2cm × 2.5cm)
Concentration of CoCl ₂	0.2 – 0.5M
Temperature	323 – 383K
Applied Voltage	2.4 – 3.3V
Time	2 hours
Electrodes Distance	2 cm

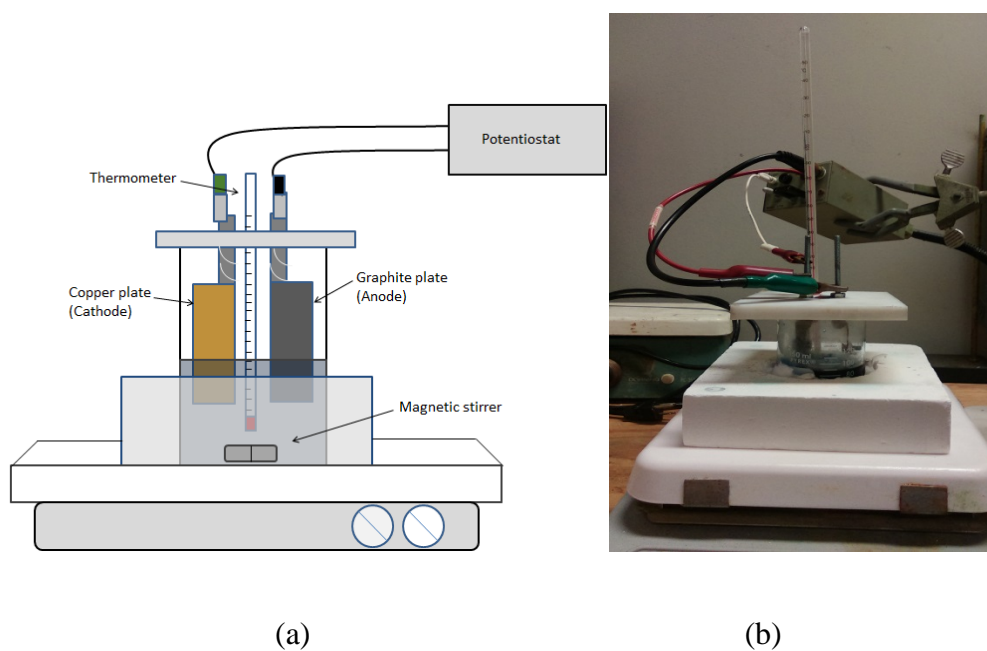


Figure 4.6. (a) Schematic and (b) actual electrodeposition setup.



(a)

(b)

Figure 4.7. Photographs of (a) the copper cathode and (b) the cobalt deposited copper cathode.

4.3.3 SEM Analysis

Scanning Electron Microscopy (SEM, JEOL 7000, Japan) was used to analyze the surface morphology of the deposited cobalt on copper cathodes. Each sample was cut into appropriate size to fit a sample stub for SEM. The cutting samples were stuck to the sample stub using carbon conducting tape and were inserted to the chamber of SEM. The magnification of SEM image was $1000\times$, and the accelerating voltage was 20kV. The working distances of the image were 10mm for the surface of samples and 8 mm to 10mm for the cross-sectional area of samples, respectively.

4.3.4 XRD Analysis

The elemental analysis of cobalt deposits from the samples were done with Bruker D8 XRD using $\text{Co } k\alpha$ radiation. In order to acquire more amounts of cobalt deposits, two new experiments with different parameters were performed for 6 hours. One sample was the cobalt deposit on the copper sheet and the other sample was the cobalt deposit powder from

the magnetic stirrer. Each sample was mounted on the sample holder and was run with the equipment. The result pattern peaks were analyzed and compared with ICDD card.

Table 4.3. Parameters of the samples to use the elemental analysis with XRD.

Parameters	Sample	
	Co on copper cathode	Co deposit powder
Working Electrode	Cu ($2\text{ cm} \times 2.5\text{ cm}$)	Cu ($2\text{ cm} \times 2.5\text{ cm}$)
Counter Electrode	C ($2\text{ cm} \times 2.5\text{ cm}$)	C ($2\text{ cm} \times 2.5\text{ cm}$)
Concentration of CoCl_2	0.5M	0.5M
Temperature	323K	363K
Applied Voltage	2.7V	3.3V
Time	6 hours	6 hours
Electrodes Distance	2 cm	2 cm

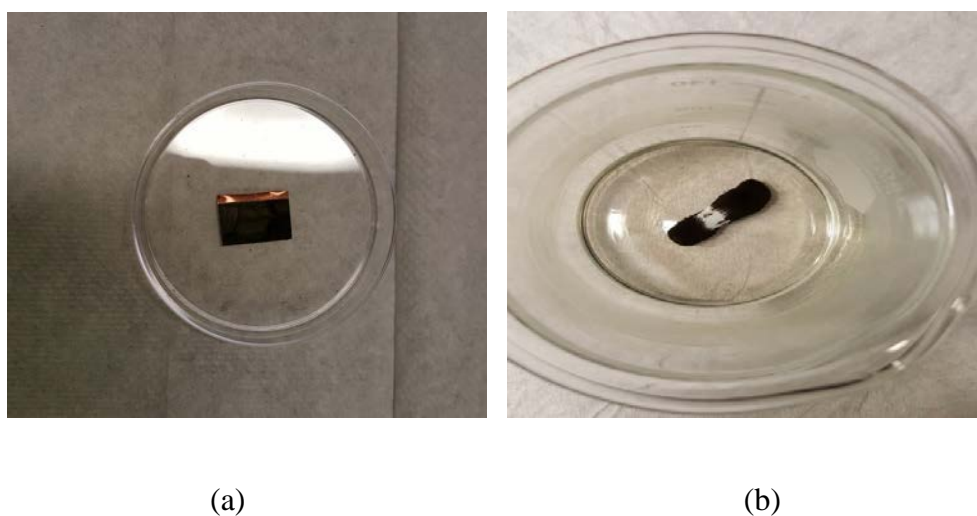


Figure 4.8. Images of (a) the Co deposits on the copper cathode and (b) the Co deposit powders stuck on a magnetic stirrer from 6 hour experiments.

CHAPTER 5

RESULTS AND DISCUSSION

5.1 Cyclic Voltammetry (CV)

To study the electrode reaction such as the electron transportation in the ionic liquid, the cyclic voltammetry test was performed at 323K. As shown in Figure 5.1, the cathodic limit which generates the hydrogen cathodic gas[60] is about -1.2V at 323K. Figure 5.2 shows the CV curve of 0.2M CoCl₂ Urea/ChCl mixture according to the different scan rates. As the scan rate increases, the cathodic reduction potential becomes more negative, which indicates the irreversible process takes place. For the irreversible process, the transfer coefficient can be calculated by the following equation [54]:

$$|E_p - E_{p/2}| = 1.857RT/\alpha nF \quad (5.1)$$

where E_p is the cathodic potential in V, $E_{p/2}$ is the half of cathodic potential in V, R is the gas constant which is 8.314 J/K•mol, T is the temperature in K, α is the transfer coefficient, n is the number of exchanging electrons, and F is the Faraday constant, 96500 C/mol. Using the equation above and the data from Figure 5.2, the average transfer coefficient is 0.22.

To calculate the diffusion coefficient of cobalt ion in the electrolyte at 323K, the data from Figure 5.2 [52]:

$$I_p = 0.4958nAc^i \left(\frac{\alpha nF}{RT}\right)^{1/2} D^{1/2} \nu^{1/2} \quad (5.2)$$

where I_p is the cathodic peak current in A, A is the electrode area in cm^2 , c^i is the initial concentration in mol/cm^3 , α is the transfer coefficient, D is the diffusion coefficient in cm^2/s and v is the scan rate in V/s . The calculated diffusion coefficient is $3.38 \times 10^{-6} \text{cm}^2/\text{s}$ using Figure 5.3. Table 5.1 lists the transfer coefficient and the diffusion coefficient in various ionic liquid systems. According to Table 5.1, the calculated values are reasonable as compared with the literature data in the same ionic liquid system with different temperatures.

Table 5.1. The transfer coefficient and the diffusion coefficient in various ionic liquid systems.

System	T (K)	α	D (cm^2/s)	Reference
CoCl ₂ in Urea/ChCl	323	0.22	3.38×10^{-6}	This work
CoCl ₂ in Urea/ChCl	373	0.36	1.7×10^{-6}	[53]
CoCl ₂ in urea-NaBr-KBr	373	0.45	2.5×10^{-6}	[61]
CoCl ₂ in urea-NaBr-acetamide	353	0.26	2.83×10^{-7}	[62]
CoCl ₂ in urea-NaBr-acetamide	353	0.23	2.24×10^{-7}	[63]
Co(BF ₄) ₂ in BMIMBF ₄	333	0.18	1.76×10^{-8}	[64]
Co(BF ₄) ₂ in BMIMBF ₄	353	-	7.6×10^{-8}	[65]
Co(TFSA) ₂ in BMPTFSA	300	-	7.2×10^{-8}	[66]
CoCl ₂ in AlCl ₃ -EMIC	295	-	4.40×10^{-7}	[67]
ZnO in Urea/ChCl	373	0.2	1.89×10^{-8}	[39]
PbO in Urea/ChCl	363	0.52	1.42×10^{-7}	[41]
AlCl ₃ in BMIC	363	-	2.2×10^{-7}	[68]
AlCl ₃ in EMIC	363	-	9.1×10^{-7}	[69]

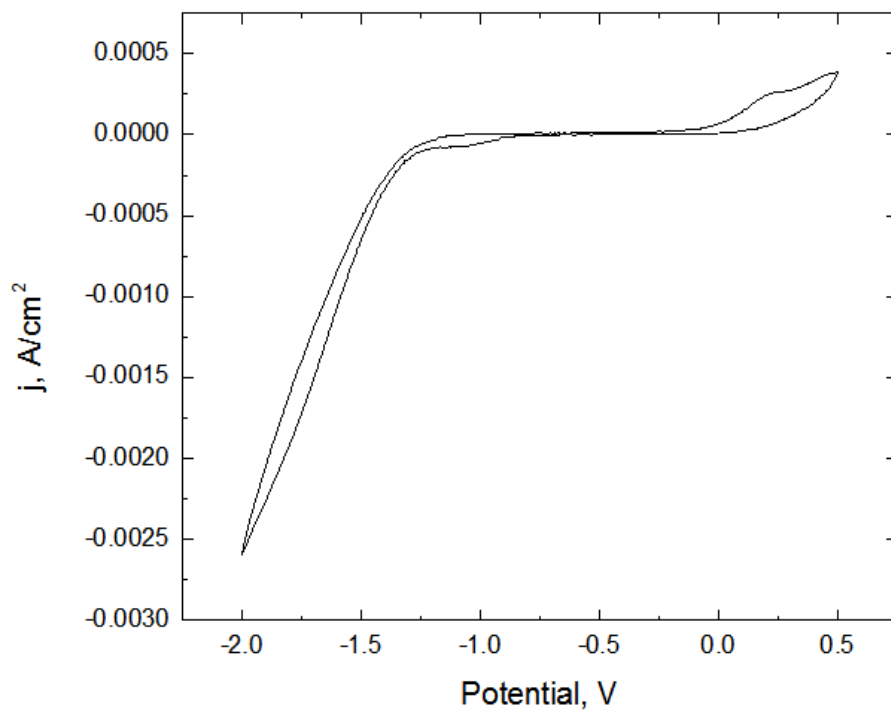


Figure 5.1. Cyclic voltammogram of Urea/ChCl (2:1 ratio) with 50 mV/s scan rate at 323K.

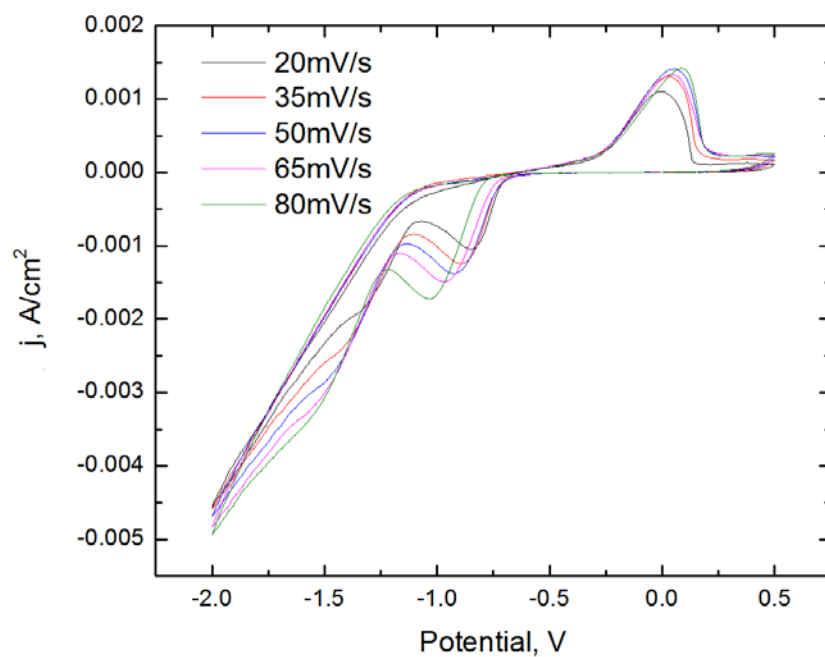


Figure 5.2. Cyclic voltammogram of 0.2M CoCl_2 -Urea/ChCl according to the various scan rates at 323K.

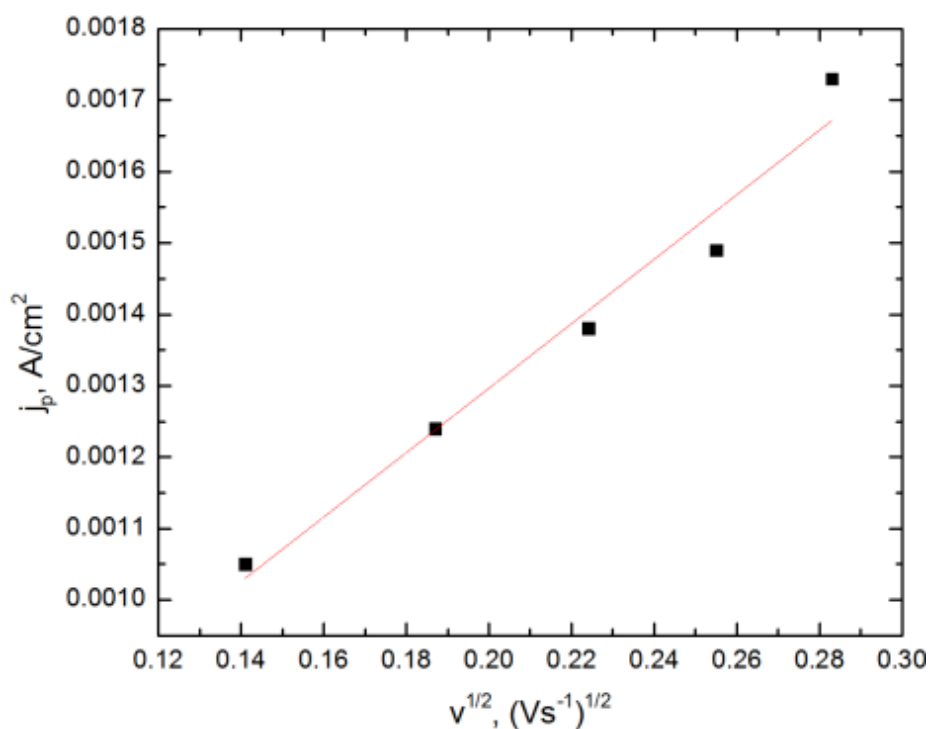


Figure 5.3. Cathodic current density peaks from cyclic voltammogram of 0.2M CoCl₂-Urea/ChCl as a function of various scan rates at 323K .

5.2 The Effect of Temperature on the Electrodeposition of Co

To determine the effect of temperature on the electrodeposition of cobalt on the copper cathode, four experiments were performed under the fixed cell voltage, concentration of CoCl₂, and time. Based on the data from the experiments, the current density plot, the current efficiency, and the energy consumption were calculated. Figure 5.3 shows that the current density decreases rapidly at the initial 40 seconds and then increases gradually. When the current density increases to some value, it begins to be stable. As the heating temperature increases, the current density increases because the diffusion rate increases with temperature, which increases the ion transportation near the copper substrate. The lower viscosity of the

electrolyte with increasing temperature would also cause higher current density at higher temperature.

The current efficiency and the energy consumption at different temperatures are summarized in Table 5.2. The current efficiency according to the temperature is ranged from 76.78% to 78.55%. Thus there exists no significant difference in the current efficiency according to the temperature. The current efficiency at 323K is greater than other values and thus the energy consumption at 323K is the lowest.

The surface morphology of the cobalt deposited on the copper cathode at different temperatures was studied using SEM. In Figure 5.4, all micrographs show the clustered particles that are uniformly layered on copper substrates. The size of cobalt particles at 323K is relatively small compared with that of the other depositions at higher temperatures. As the temperature increases, cobalt particles become larger but remain spherically. Figure 5.5 shows the cross-sectional Co deposits at 323K and 383K under the concentration 0.2M, 3.0V and 2 hours. It can be seen that the cobalt deposition is uniformly distributed on the copper cathodic electrode. Also, the dependence of the particle size in the cross-sectional area on the temperature (Figure 5.5) is similar to that in the surface morphology of the cobalt deposition (Figure 5.4).

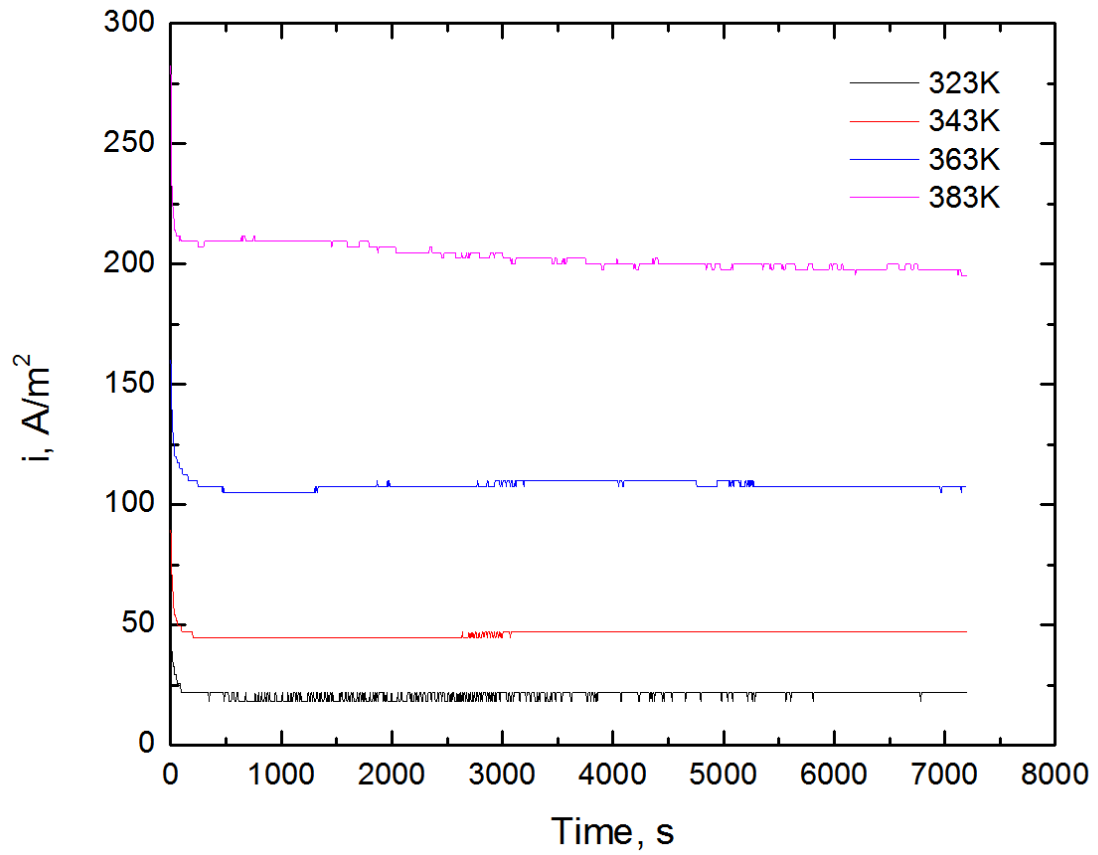
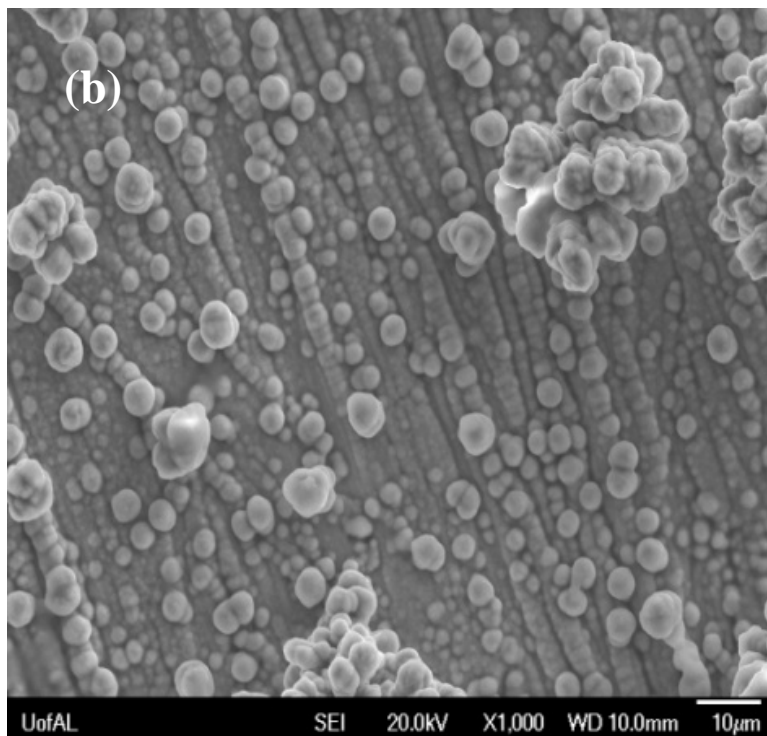
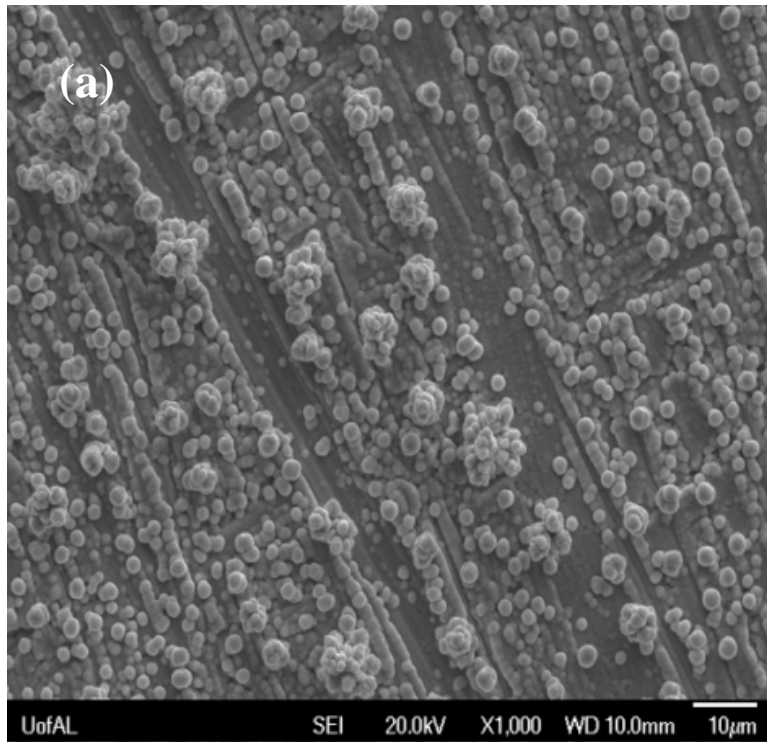


Figure 5.4. Current density as a function of time at various temperatures under the applied voltage 3.0V and concentration 0.2M of CoCl_2 .

Table 5.2. Summary of the current efficiency and the energy consumption according to temperature. (Concentration of $\text{CoCl}_2 = 0.2\text{M}$, Cell volatage = 3.0 V)

Temperature (K)	η (%)	E (kWh/kg)
323	78.58	3.47
343	76.78	3.55
363	78.22	3.49
383	77.62	3.52



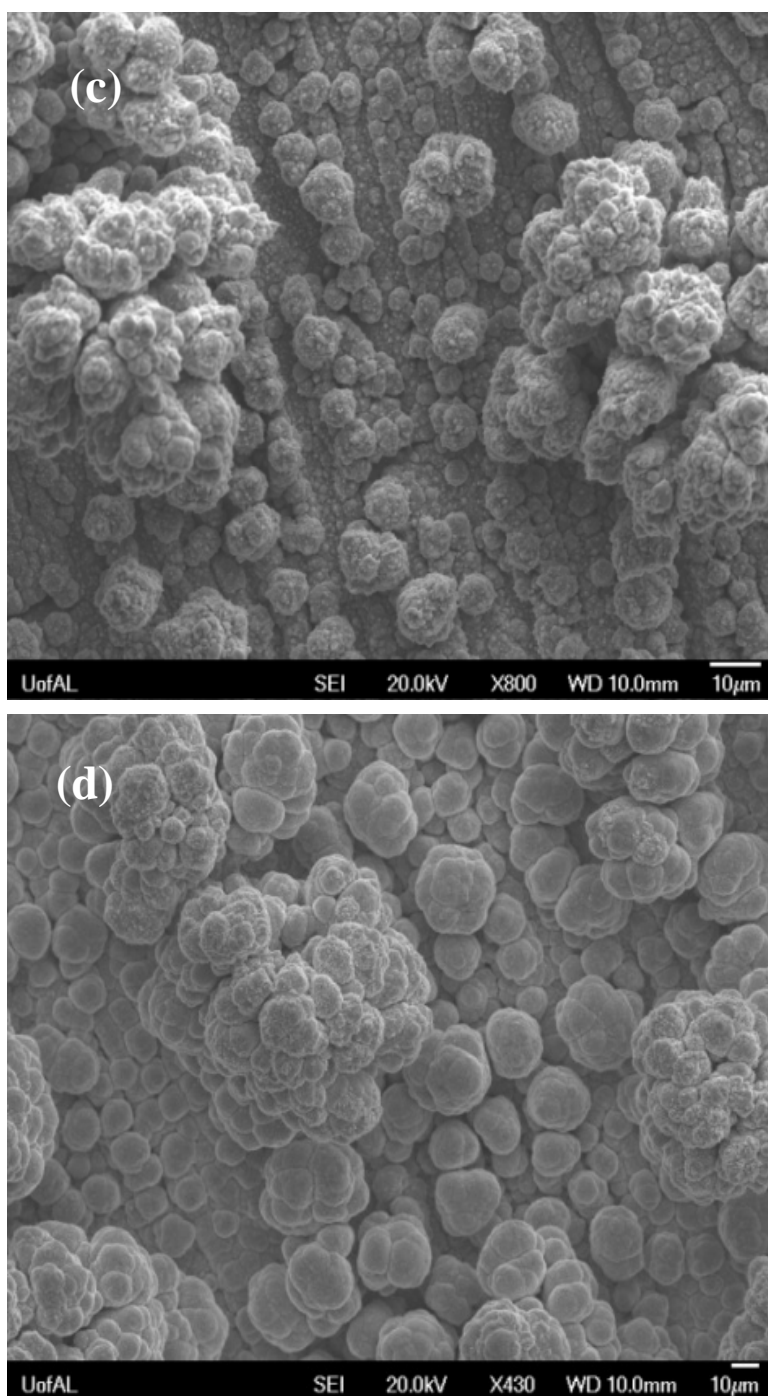


Figure 5.5. SEM micrographs of Co electrodeposits at (a) 323K, (b) 353K, (c) 363K, (d) 383K under the applied voltage 3.0V, concentration 0.2M of CoCl_2 and 2 hours.

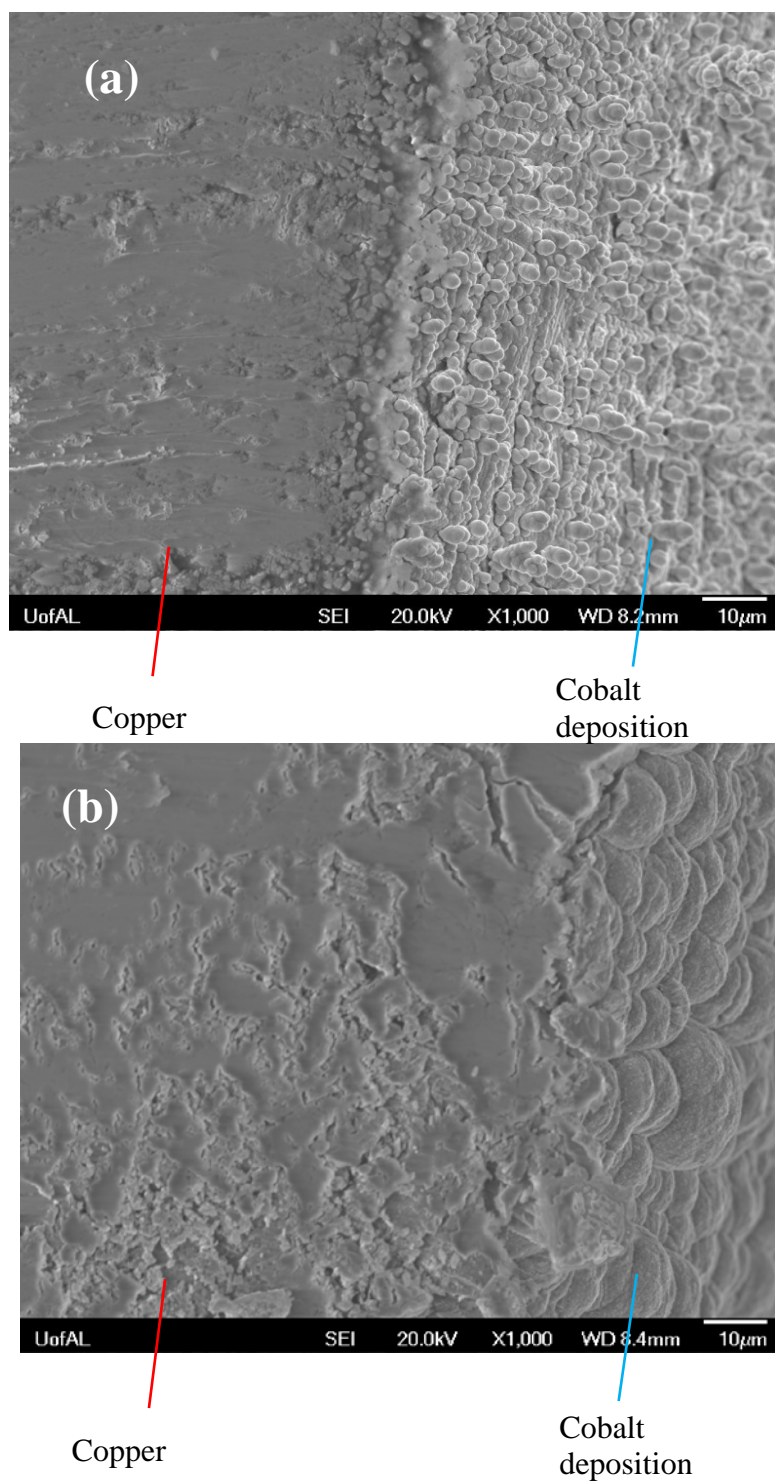


Figure 5.6. SEM micrographs of cross-sectional Co electrodeposits at (a) 323K and (b) 383K under the applied voltage 3.0V, concentration 0.2M of CoCl_2 , and 2 hours.

5.3 Effect of the Applied Voltage on the Electrodeposition of Co

The effect of the cell potential on the cathode for the electrodeposition of cobalt was studied by the current density plot, calculating the current efficiency and the energy consumption, and the surface morphology using SEM and XRD patterns. The current density as a function of time at 353K, 0.2M of CoCl_2 for 2 hours with different applied voltage was plotted as seen in Figure 5.6. The highest current density is observed at 3.3V while the current density at 2.4V is the lowest. As the larger cell potential is applied, the higher current density is obtained. This might be due to the larger reduction potential on the cathode surface as the larger cell voltage is applied.

The current efficiency and the energy consumption according to the cell voltage are summarized in Table 5.3. The current efficiency increases as the cell voltage increases from 2.4V to 2.7V. However, there is a huge current efficiency drop at 3.0V because the ionic liquid was decomposed during the experiment. Also, the dendrite formation would be another reason for decreasing current efficiency at the greater cell voltage. The energy consumption at 2.4V is only 2.61 kWh/kg, which is the lowest value compared with others. The energy consumption increases at 3.0V significantly and then continues to be greater.

The surface morphology on the copper cathode according to the applied voltage was examined using SEM in Figure 5.7. The deposition at the applied voltage 2.4V is compact and uniformly layered without particles and clusters. At 2.7V~3.0V, the micrographs show the nodular shape of particles and clusters and the similar particle size. However, the cluster size at 3.0V is larger than that at 2.7V. At 3.3V, the dendrite forms on the uniform and dense cobalt deposition as a background. The cross-sectional morphologies of Co deposition at 2.4V and 3.3V are shown in Figure 5.8. No particle is shown on the copper substrate.

However, the boundary between the copper and the cobalt deposits shows that the cobalt was layered uniformly on the copper electrode at 2.4V. At 3.3V, a few dendrites in the circle in Figure 5.8b are observed but not uniformly distributed. This resulted from the loss of the dendrites when the deposited sample was cut to prepare the specimen for the SEM. However, the dendrites were observed in other spots far from the cut area, as shown in Figure 5.9, where the average size of the cobalt dendrites was measured as $156\mu\text{m}$.

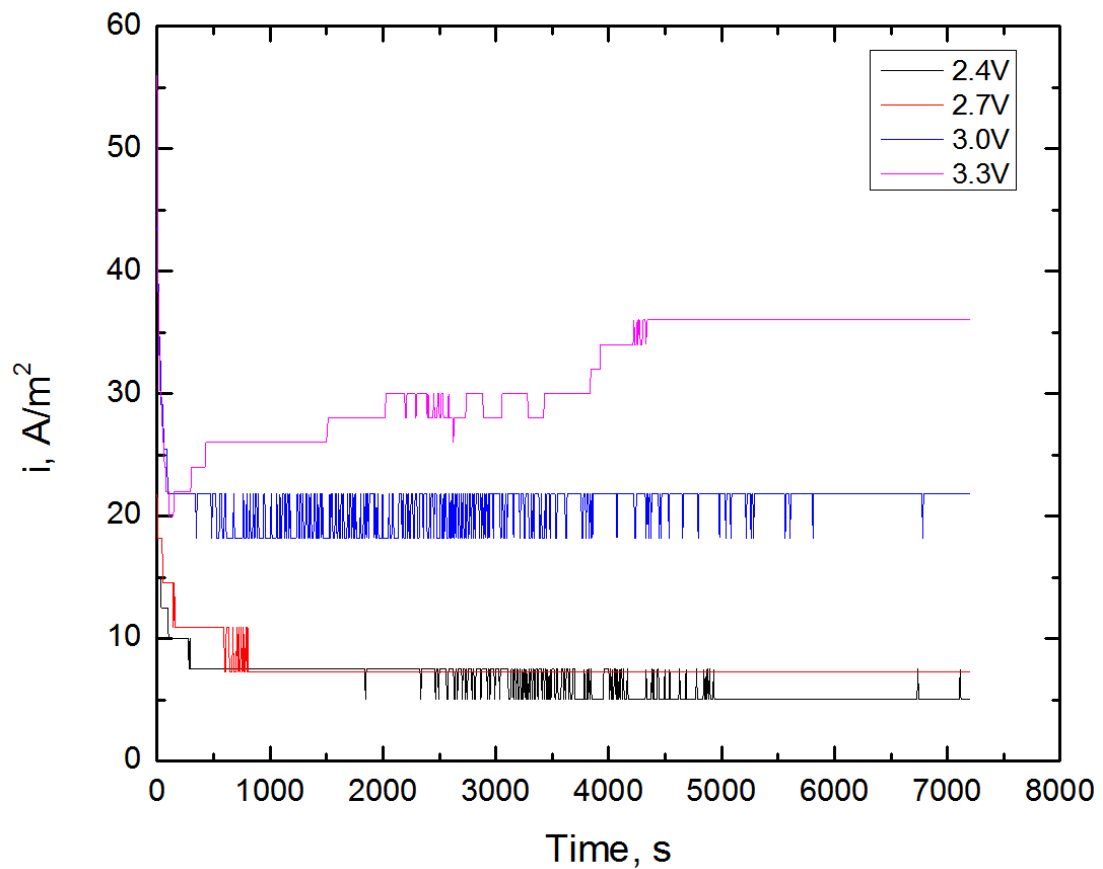
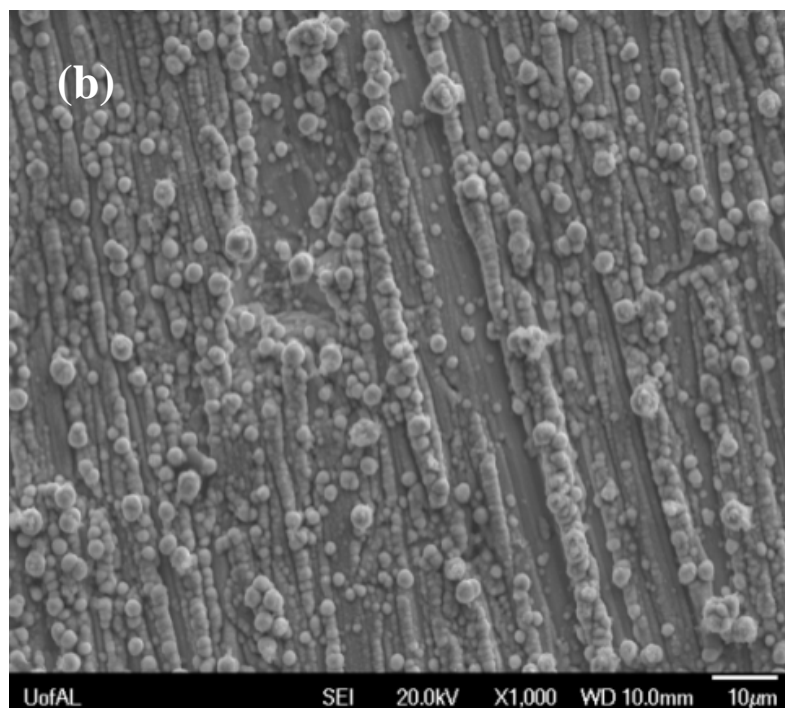
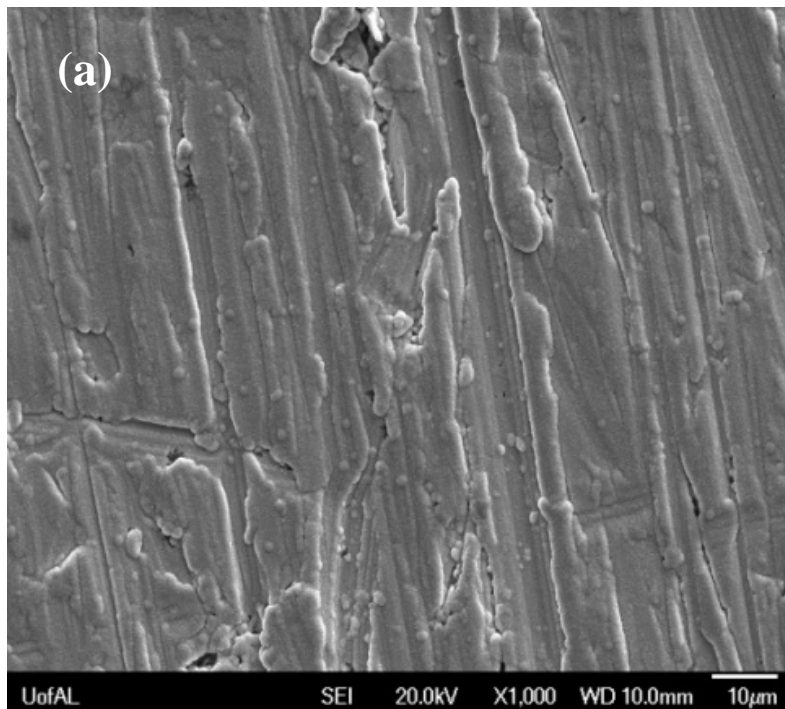


Figure 5.7. Current density as a function of time at the different applied voltage under the temperature 323K and concentration 0.2M of CoCl_2 .

Table 5.3. Summary of the current efficiency and the energy consumption according to the reduction potential. (Concentration of $\text{CoCl}_2 = 0.2\text{M}$, Temperature = 323K)

Cell Voltage (V)	η (%)	E (kWh/kg)
2.4	83.64	2.61
2.7	87.92	2.79
3.0	78.58	3.47
3.3	73.54	4.08



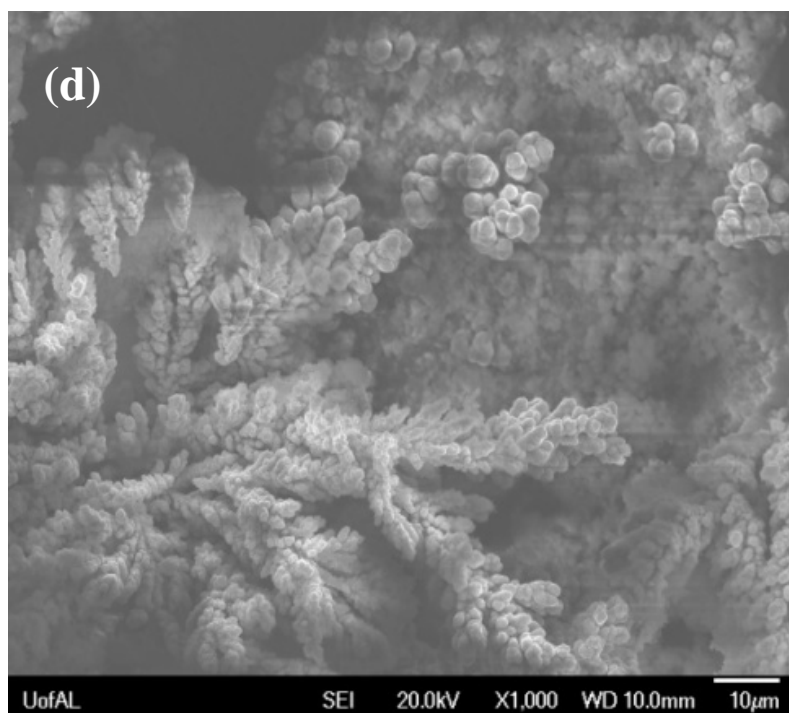
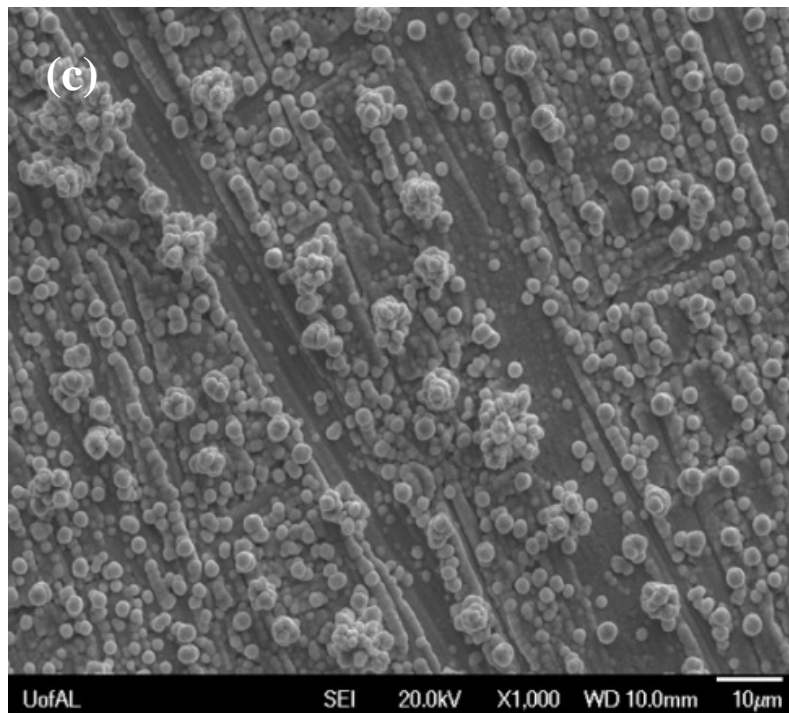


Figure 5.8. SEM micrographs of Co electrodeposits at the applied voltages (a) 2.4V, (b) 2.7V, (c) 3.0V, (d) 3.3V under the temperature 323K, concentration 0.2M of CoCl_2 and 2 hours.

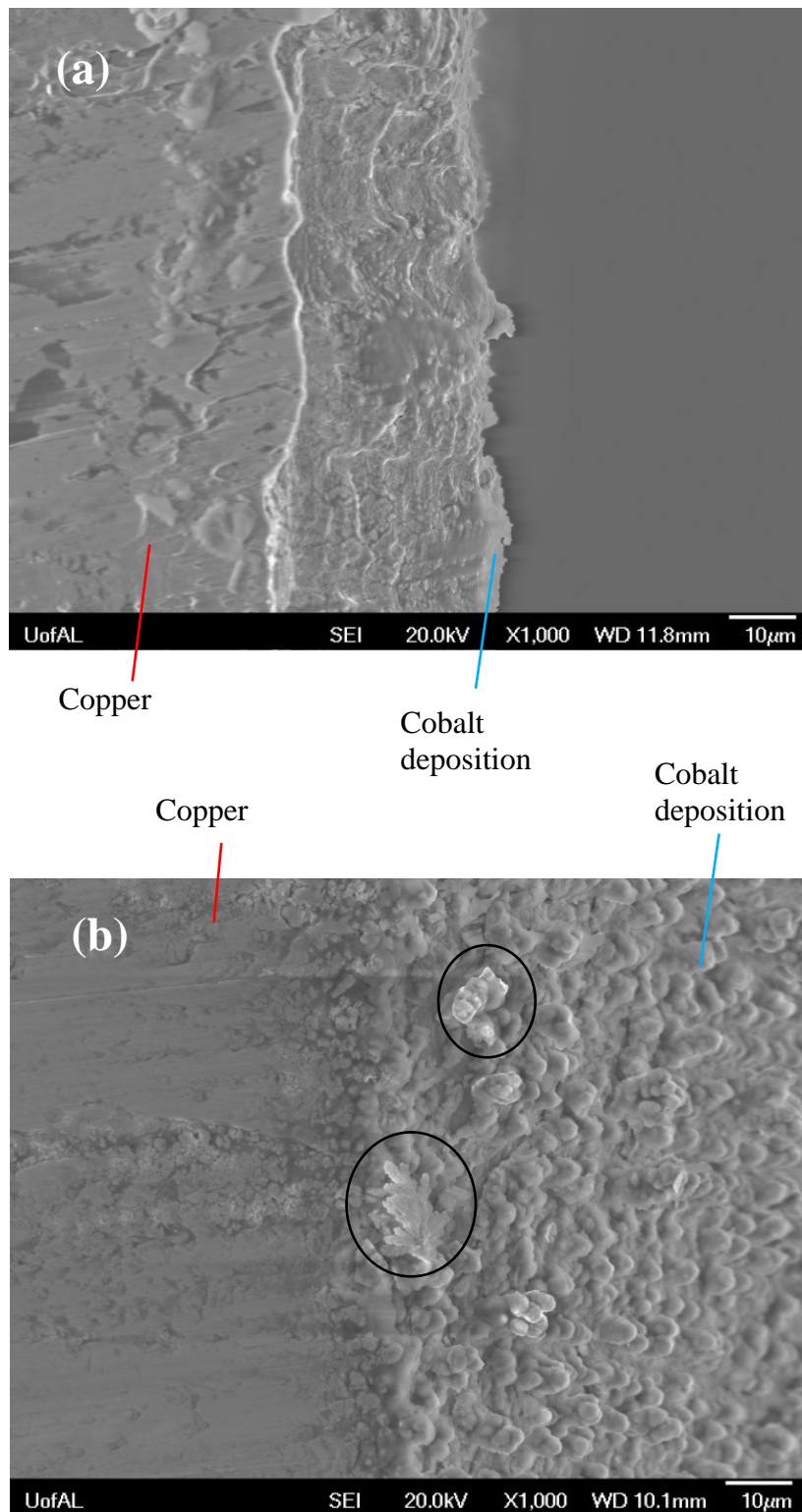


Figure 5.9. SEM micrographs of cross-sectional Co electrodeposits according to the applied voltages (a) 2.4V and (b) 3.3V under the temperature 323K, concentration 0.2 M of CoCl_2 and 2 hours.

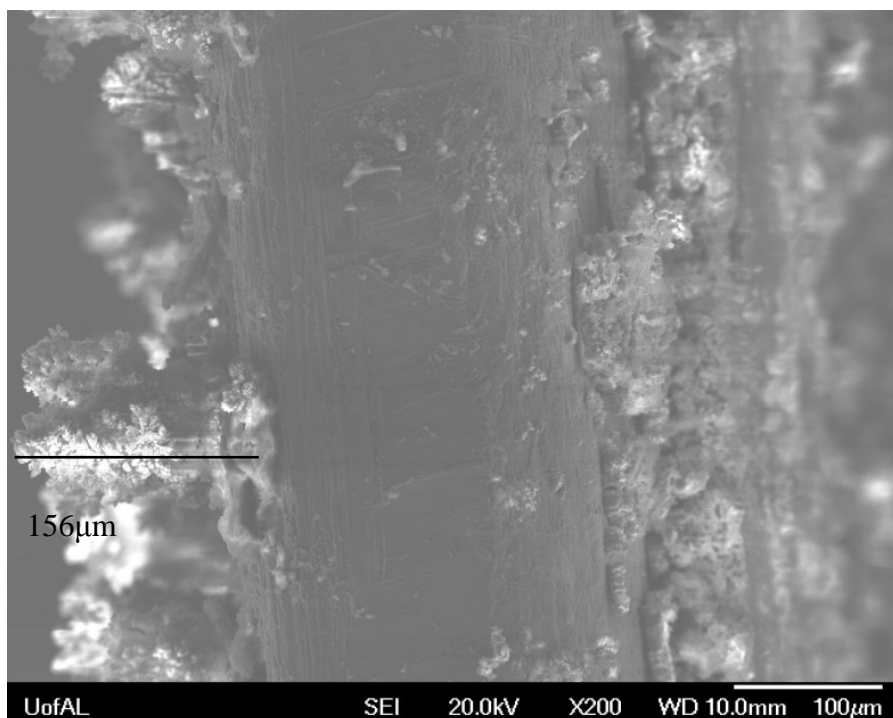


Figure 5.10. SEM micrographs of the single dendrite of Co electrodeposits under the temperature 323K, concentration 0.2M of CoCl_2 , the applied voltage 3.3V, and 2 hours.

5.4 Effect of the Concentration of CoCl_2 on the Electrodeposition of Co

The effect of the concentration on the electrodeposition of cobalt with different concentration of CoCl_2 was investigated using the current density plot, the calculation of the current efficiency and the energy consumption, and the surface morphology using SEM and XRD patterns. As shown in Figure 5.10, there is not much difference between results from 0.2M to 0.5M of CoCl_2 . However, the current density at 0.5M of CoCl_2 is still higher than lower concentration values. The trend in this current density plot shows that the current density increases at higher concentration. This might be due to more reducible ions in the higher concentration electrolytes.

The calculated current efficiency and energy consumption are listed in Table 5.4. As the concentration of CoCl_2 increases from 0.2M to 0.3M, the current efficiency increases with small amount. The current efficiency increases at 0.5M significantly. The saturation was observed when 0.6M CoCl_2 -Urea/ChCl solution was synthesized. This indicates that 0.5M is about maximum concentration in this system. That might cause the sudden increase of current efficiency at 0.5M. Energy consumption at 0.5M with the same temperature and cell voltage is relatively lower than other data. The low temperature and the low applied voltage lead to the smaller total charge for the lower energy consumption. The optimized energy consumption in this work is 2.59 kWh/kg at 0.5M.

The microstructures of the cobalt deposition on the copper substrate with different CoCl_2 concentrations were analyzed using SEM, as shown in Figure 5.11. The shapes of the depositions at the CoCl_2 concentrations 0.2M and 0.3M are really similar to each other although more particles and clusters are appeared under the 0.3M concentration. However, in the surface morphology at 0.5M, particles are rounded with slightly larger size. The cross-sectional morphology is determined, as shown in Figure 5.12, according to the concentration of electrolytes under 2.7V, 323K, and 2 hours. In Figure 5.12a of 0.3M CoCl_2 , the spherical particles are observed on the copper electrode. In Figure 5.12b of 0.5M CoCl_2 , the shape of particles in the formation of cobalt deposition is spherical as well as the particles in Figure 5.12a. However, the Co deposition layer without the particles at 0.5M (Figure 5.12b) might be thicker than that at 0.3M (Figure 5.12a). As the concentration of the ions increases at the cathode, the growth of the cobalt deposited layer forms the large grains by diffusion.

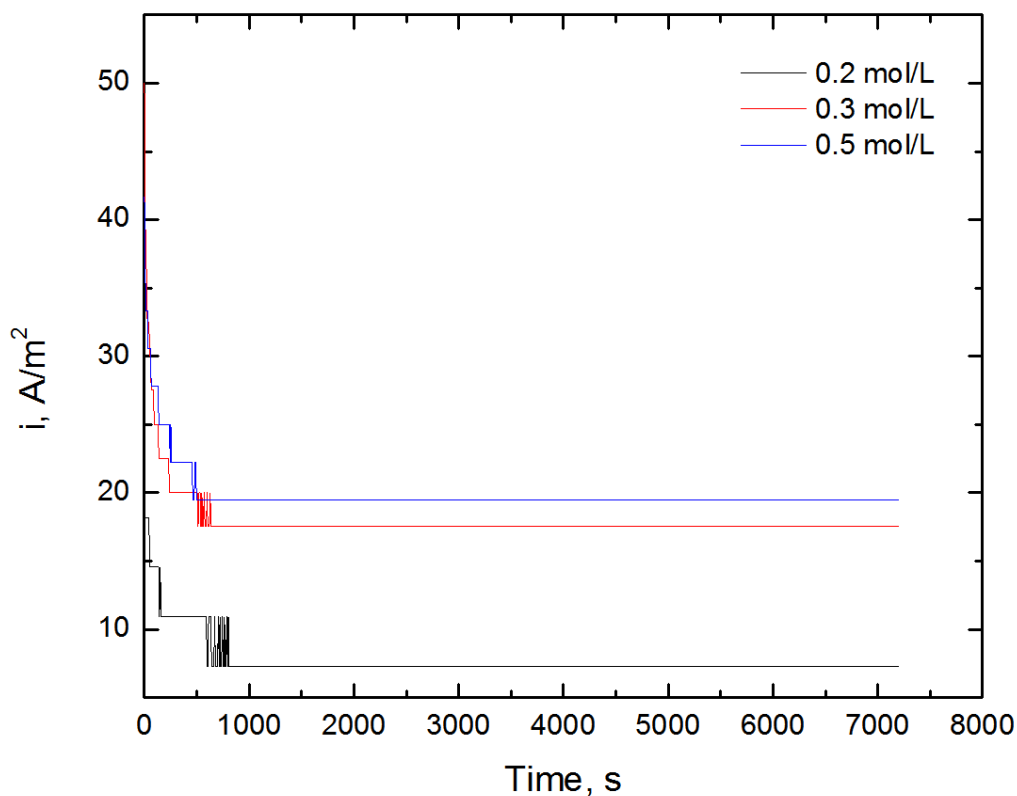
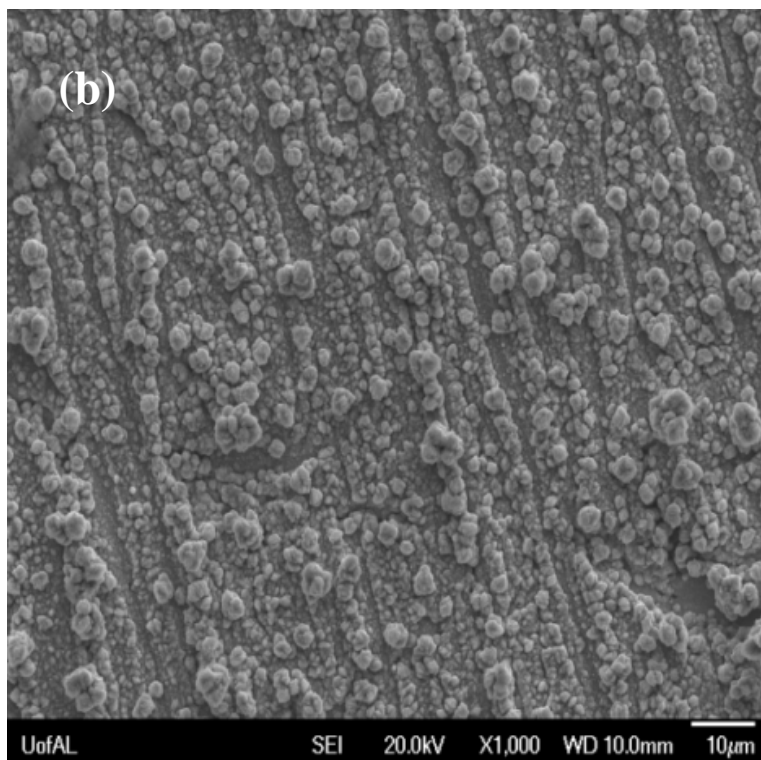
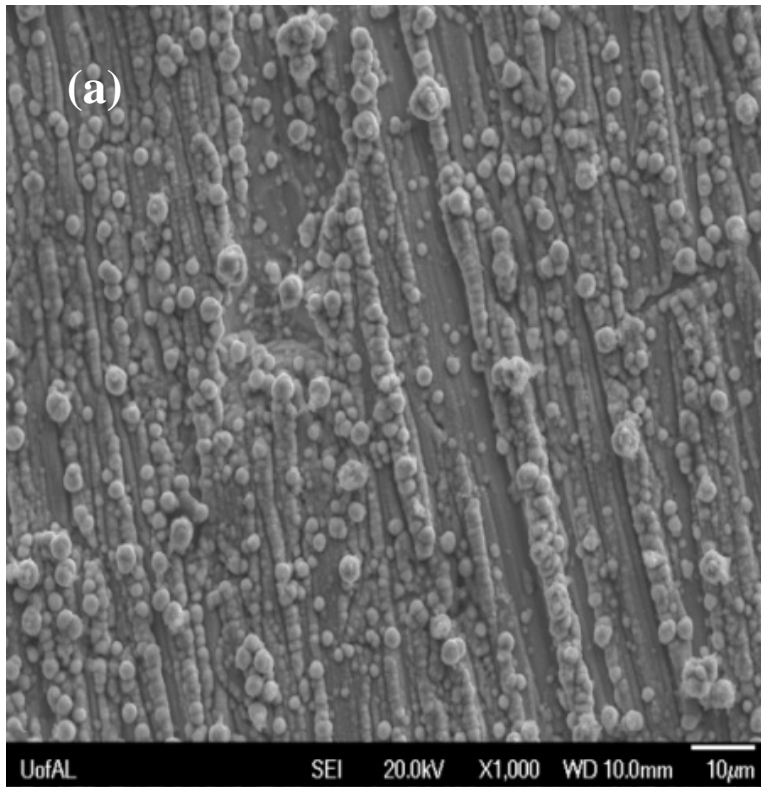


Figure 5.11. Current density as a function of time at the different concentrations of CoCl_2 under the applied voltage 2.7 V and temperature 323K.

Table 5.4. Summary of the current efficiency and the energy consumption according to the concentration of CoCl_2 . (Temperature = 323K, Cell volatage = 2.7V)

Concentration of CoCl_2 (M)	η (%)	E (kWh/kg)
0.2	87.92	2.79
0.3	85.06	2.89
0.5	95.00	2.59



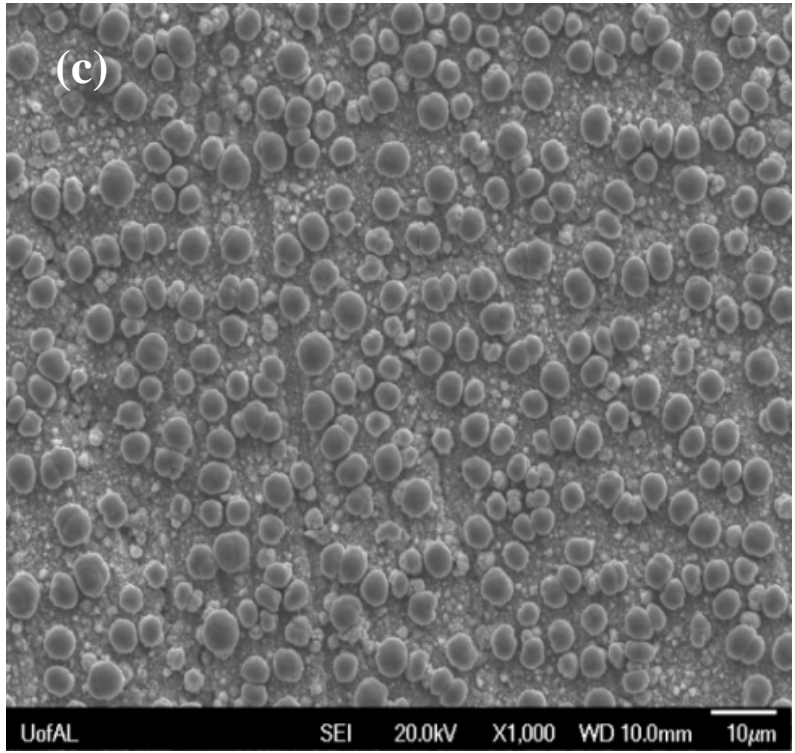
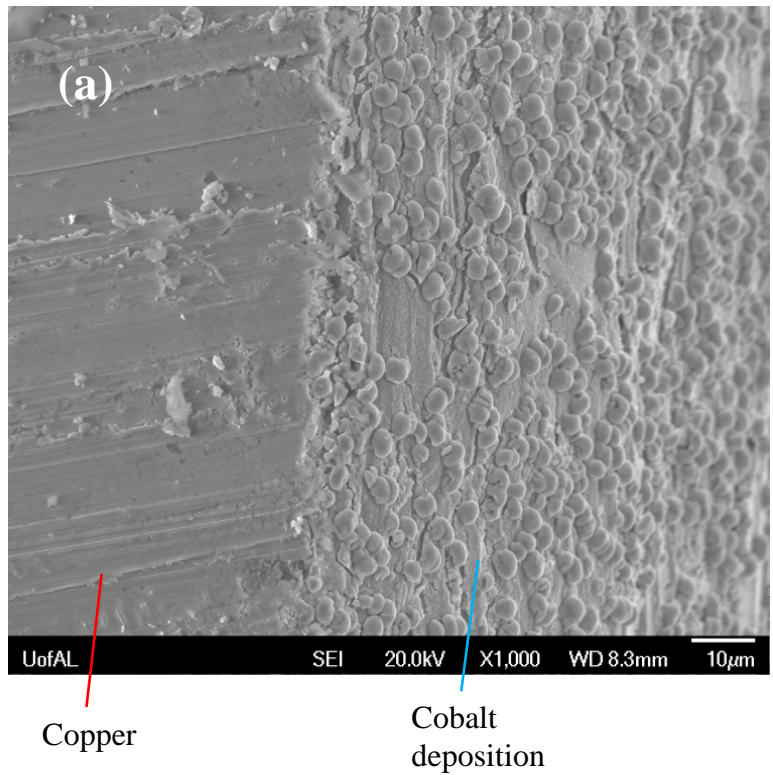


Figure 5.12. SEM micrographs of Co electrodeposits according to the concentration of CoCl_2 (a) 0.2M, (b) 0.3M, (c) 0.5M under the applied voltage 2.7 V, the temperature 323K and 2 hours.



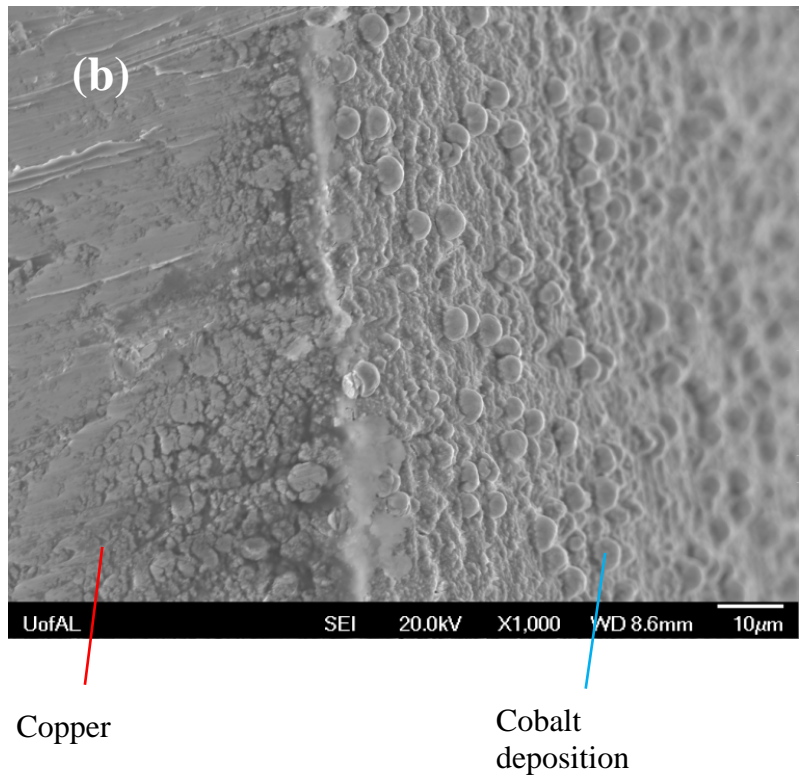


Figure 5.13. SEM micrographs of the cross-sectional Co electrodeposits according to the concentration of CoCl_2 (a) 0.3M and (b) 0.5M under the applied voltage 2.7V, temperature 323K and 2 hours.



Figure 5.14. Saturated 0.6M CoCl_2 -Urea/ChCl solution

5.5. Chemical Element Analysis of the Co Deposit

To determine the chemical elements of Co deposits, XRD pattern was used for two samples from the 6 hour experiments. One was the Co-deposited on Cu cathode and the other was the pure Co powder from the experiments. As shown in Figure 5.14, the used parameters are the same as those in the previous experiments except the performing time. In Figure 5.14a, the peaks from two elements, cobalt (ICDD File #04-001-3273) and copper (ICDD File #00-004-0936), are shown. These peaks are from the substrate copper and the cobalt deposits. To confirm the purity of Co deposition, the applied voltage 3.3V was used to obtain an easily detachable cobalt deposit due to the formation of dendrites (Figure 14b). Hence, the cobalt powders stuck on the magnetic stirrer were collected after the experiment. The Co deposits proved to be highly pure without any other elements since only cobalt peaks appeared, as shown in Figure 5.14b.

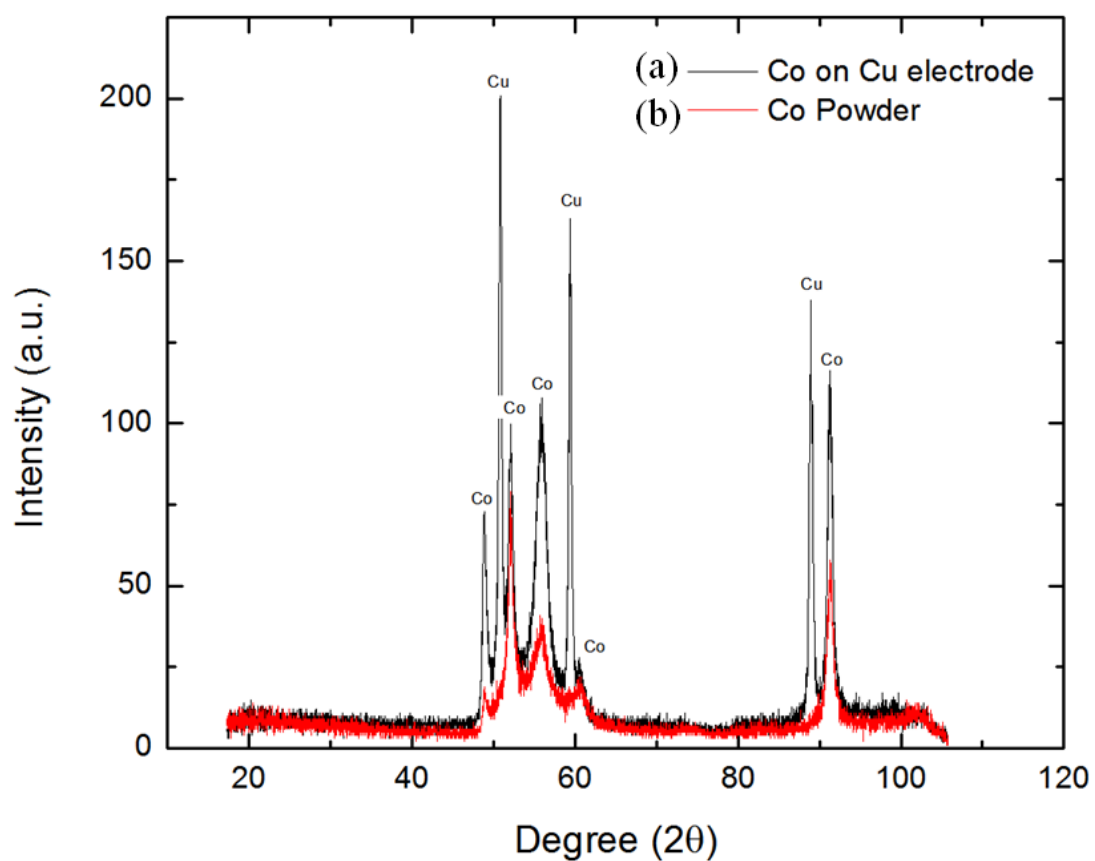


Figure 5.15. XRD pattern of the Co electrodeposits for 6 hours under the concentration 0.5M of CoCl_2 at (a) the applied voltage 3.3V and temperature 363K and (b) applied voltage 2.7V and temperature 323K under the concentration 0.2M of CoCl_2 for 6 hours.

CHAPTER 6

CONCLUSION

To obtain the high purity cobalt deposit with high efficiency, the effect of temperature, cell voltage, and CoCl_2 concentration on the electrodeposition of cobalt in Urea/ChCl (2:1 ratio) was investigated using current density, current efficiency, and energy consumption. XRD pattern and SEM micrograph were used to characterize the cobalt deposition. The experiment of electrodeposition of cobalt from the cobalt solutions with the urea and the choline chloride had been performed for 2 hours with variation of temperatures, cell voltages, and concentrations of CoCl_2 .

The cyclic voltammetry was tested with 0.2M CoCl_2 using various scan rates to determine the reduction potential in Urea/ChCl at 323K, which was the temperature of the lowest energy consumption. The curve of cyclic voltammetry shows that the reduction of Co(II) to Co is an irreversible process with one step, 2 electrons transport. Based on the data from cyclic voltammetry test, the transfer coefficient of Co(II) and the diffusion coefficient were calculated as 0.22 and $3.38 \times 10^{-6} \text{cm}^2/\text{s}$, which were reasonable as compared with the literature.

Under the applied voltage 3.0V and concentration 0.2M of CoCl_2 , the current efficiency with the temperature range of 323K to 383K didn't change significantly but still the highest current efficiency (78.58%) was observed at 323K with the lowest energy consumption (3.47 kWh/kg).

Under the temperature 353K and concentration 0.2M of CoCl_2 , the change of the applied voltage showed the lowest energy consumption (2.61kWh/kg) at 2.4V with current efficiency 83.64%. The higher applied voltage caused the lower current efficiency due to the formation of dendrites in the cobalt deposition.

Under the temperature 323K and cell voltage 2.7V, increasing the concentration of CoCl_2 showed the highest current efficiency (95%) with the lowest energy consumption (2.59 kWh/kg) at concentration 0.5M of CoCl_2 , which was about maximum concentration in the present system.

SEM images showed the surface morphology of cobalt deposits on the copper cathodes according to the different parameters. As the temperature increases, the particles in the cobalt deposits grew larger without changing their shape. Under the temperature 323K and concentration 0.2 M of CoCl_2 , the higher applied voltage showed the dendrite on the surface of the copper sheet at 3.3V and the measured average size of the dendrites was 156 μm . Under the applied voltage 2.7 V and the temperature 323K, increasing the concentration of CoCl_2 didn't show the large change of the particle size except for the thicker coverage of cobalt layer.

The elemental analysis in the cobalt deposits was performed using XRD for 6 hour experiments to obtain a larger amount of samples. The XRD peaks of cobalt deposit powders were the same as the pure cobalt peaks (ICDD File #04-001-3273), which confirmed the pure cobalt without any other elements.

REFERENCES

- [1] F. Habashi, "Recent Trends in Extractive Metallurgy," *J. Min. Metall. Sect. B Metall.* **45** (2009), pp1-13.
- [2] N. Greenwood, A. Earnshaw, *Chemistry of the Elements*, 2nd Edition, Oxford, Butterworth-Heinemann (1997), pp. 1113-1120.
- [3] M. Hawkins, "Why we need cobalt," *Applied Earth Science: Transactions of the Institution of Mining & Metallurgy, Section B* **110** (2001), pp66–71.
- [4] M.R. Ali, A. Nishikata, T. Tsuru, "Electrodeposition of Co-Al alloys of different composition from the AlCl_3 -BPC- CoCl_2 room temperature molten salt," *Electrochim. Acta* **42** (1997), pp. 1819-1828.
- [5] M.J. Donachie, S.J. Donachie, *Superalloys: A Technical Guide*, ASM International (2002).
- [6] R. Michel, M. Nolte, M. Reich, F. L er, "Systemic effects of implanted prostheses made of cobalt-chromium alloys," *Archives of Orthopaedic and Trauma Surgery* **110** (1991), pp. 61–74.
- [7] J.A. Disegi, *Cobalt-base Alloys for Biomedical Applications*, ASTM International (1999), pp. 62-70.
- [8] K.G. Fisher, Cobalt processing developments, The Southern African Institute of Mining and Metallurgy, 6th Southern African Base Metals Conference (2011), pp.237-258.
- [9] A.Z. Ahmed, Energy Conservation, In *Tech.* October (2012), pp.149-170.
- [10] R. David. Wilburn, Cobalt Mineral Exploration and Supply From 1995 Through 2013, pp.1-16.
- [11] Best Available Techniques (BAT) Reference Document for the Non-Ferrous Metal Industries, Joint Research Centre (2014), pp.899-900.
- [12] F. Endres, A.P. Abbott, D. R. Macfarlane, "Electrodeposition from Ionic Liquids." Wiley VCH (2008), pp. 1633–1634.
- [13] P. Wasserscheid, T. Welton, *Ionic Liquids in Synthesis*, Wiley-VCH Verlag GmbH & Co. KGaA (2002), pp.12-56.

- [14] A.P. Abbott, K.S. Ryder, U. Konig, "Electrofinishing of metals using eutectic based ionic liquids," *Trans. Inst. Met. Finish* **86** (2008), pp. 196-204.
- [15] C.P. Fredlake et al., "Thermophysical Properties of Imidazolium-Based Ionic Liquids," *J. Chem. Eng. Data* **49** (2004), pp. 954-964.
- [16] S. Forsyth, J. Pringle, D. Macfarlane, "Ionic Liquids—An Overview," *Aust. J. Chem.* **57** (2004), pp. 113-119.
- [17] C. Chiappe, D. Pieraccini, "Ionic liquids: solvent properties and organic reactivity," *Journal of Physical Organic Chemistry* **18** (2005), pp. 275-297.
- [18] P. Walden, *Bull. Acad. Imper. Sci.* **68** (1914), pp. 1800.
- [19] J.S. Wilkes, J.A. Levisky, R.A. Wilson, C.L. Hussey, "Dialkylimidazolium chloroaluminate melts: a new class of room-temperature ionic liquids for electrochemistry, spectroscopy and synthesis," *Inorg. Chem.* **21** (1982), pp. 1263-1264
- [20] T.B. Scheffler, C.L. Hussey, K.R. Seddon, C.M. Kear, P.D. Armitage, "Molybdenum chloro complexes in room-temperature chloroaluminate ionic liquids: stabilization of hexachloromolybdate(2-) and hexachloromolybdate(3-)," *Inorg. Chem.* **22** (1983), pp. 2099-2100.
- [21] D. Appleby, C.L. Hussey, K.R. Seddon, J.E. Turp, "Room-Temperature Ionic Liquids as Solvents for Electronic Absorption Spectroscopy of Halide Complexes," *Nature* **323** (1986), pp. 614-616.
- [22] H.L. Chum, V.R. Koch, L.L. Miller, R.A. Osteryoung, "Electrochemical Scrutiny of Organometallic Iron Complexes and Hexamethylbenzene in a Room Temperature Molten Salt," *J. Am. Chem. Soc.* **97** (1975), pp. 3264-3265.
- [23] J. Robinson, R.A. Osteryoung, "An electrochemical and spectroscopic study of some aromatic hydrocarbons in the room temperature molten salt system aluminum chloride-n-butylpyridinium chloride," *J. Am. Chem. Soc.* **101** (1979), pp. 323-327.
- [24] J.S. Wilkes, M.J. Zaworotko, "Air and water stable 1-ethyl-3-methylimidazolium based ionic liquids," *J. Chem. Soc., Chem. Commun.* **13** (1992), pp. 965-967.
- [25] J.S. Wilkes, J.A. Levisky, R.A. Wilson, C.L. Hussey, "Dialkylimidazolium Chloroaluminate Melts: A New Class of Room-temperature Ionic Liquids for Electrochemistry, Spectroscopy and Synthesis," *Inorg. Chem.* **21** (1982), 1263-1264.
- [26] J.S. Wilkes, M.J. Zaworotko, "Air and Water Stable 1-ethyl-3-methylimidazolium Based Ionic Liquids," *J. Chem. Soc., Chem. Commun.* **13** (1992), pp. 965-967.

- [27] M. Gratzel: "Dye-Sensitized Solar Cells," *J. Photochem. Photobiol.* **C4** (2003), 145–153.
- [28] P. Bonhote, A.P. Dias, N. Papageorgiou, K. Kalyanasundaram, M. Gratzel, "Hydrophobic, Highly Conductive Ambient-temperature Molten Salt," *Inorg. Chem.* **35** (1996), pp. 1168–1178.
- [29] A.P. Abbott, G. Capper, D.L. Davies, R.K. Rasheed, V. Tambyrajah, "Novel Ambient Temperature Ionic Liquids for Zinc and Zinc Alloy Electrodeposition," *Trans IMF*, **79** (2001), pp.204-206.
- [30] A.P. Abbott, G. Capper, D.L. Davies, R.K. Rasheed, V. Tambyrajah, "Quaternary Ammonium Zinc- or Tin-containing Ionic Liquids: Water Insensitive, Recyclable Catalysts for Diels-Alder Reactions," *Green Chem.* **4** (2002), pp. 24-26.
- [31] A.P. Abbott, G. Capper, D. L. Davies, R.K. Rasheed, "Ionic Liquid Analogues Formed from Hydrated Metal Salts," *Chem. Eur. J.* **10** (2004), pp. 3769-3774.
- [32] A.P. Abbott, G. Capper, D. L. Davies, R.K. Rasheed, V. Tambyrajah, "Novel Solvent Properties of Choline Chloride/Urea Mixtures," *Chem. Commun.* **24** (2003), pp. 70-71.
- [33] A.P. Abbott, D. Boothby, G. Capper, D.L. Davies, R.K. Rasheed, "Deep Eutectic Solvents Formed between Choline Chloride and Carboxylic Acids: Versatile Alternatives to Ionic Liquids," *J. Am. Chem. Soc.* **126** (2004), pp. 9142-9147.
- [34] Q. Zhang, K. Vigier, S. Royer, F. Jerome, "Deep Eutectic Solvents: Syntheses, Properties and Applications," *Chem. Soc. Rev.* **41** (2012), pp. 7108-7146.
- [35] Qinghua Zhang, Karine De Oliveira Vigier, Se'bastien Royer, Francis Je'rome, "Deep eutectic solvents: syntheses, properties and applications," *Chem. Soc. Rev.* **41** (2012), pp. 7108-7146.
- [36] Mahi Pal, Rewa Rai, Anita Yadav, Rajesh Khanna, Gary A. Baker, Siddharth Pandey, "Self-Aggregation of Sodium Dodecyl Sulfate within (Choline Chloride + Urea) Deep Eutectic Solvent," *Langmuir* **30** (2014), pp.13191-13198.
- [37] A. Popescu, V. Constantin, M. Olteanu, O. Demidenko, K. Yanushkevich, "Obtaining and Structural Characterization of the Electrodeposited Metallic Copper from Ionic Liquids," *Rev. Chim. (Bucharest)* **62** (2011), pp. 626-632.
- [38] R.G. Reddy, "Ionic liquids: How well do we know them?," *J Phase Equilib. Diff.* **27** (2006), pp. 210–211.
- [39] H. Yang, R.G. Reddy, "Electrochemical deposition of zinc from zinc oxide in 2:1 urea/choline chloride ionic liquid," *Electrochimica Acta* **147** (2014), pp. 513–519.
- [40] H. Yang, R. G. Reddy, "Electrodeposition of zinc from zinc oxide using urea and choline chloride mixture: effect of [BMIM]HSO₄, Temperature, voltage on current efficiency,

energy consumption, and surface morphology,” TMS, Warrendale, PA, USA (2014), pp. 21-26.

[41] H. Yang, R. G. Reddy, “Fundamental Studies on Electrochemical Deposition of Lead from Lead Oxide in 2:1 Urea/Choline Chloride Ionic Liquids,” *J. Electrochem. Soc.* **161** (2014), pp. 586-592.

[42] A. Cojocaru, M. Sima, “Electrochemical Investigation of the Deposition/Dissolution of Selenium in Choline Chloride with Urea or Ethylene Glycol Ionic Liquids,” *REV. CHIM. (Bucharest)* **63** (2012), pp. 217-223.

[43] Popescu Ana-Maria, Cojocaru Anca, Donath Cristina, Constantin Virgil, “Electrochemical Study and Electrodeposition of Copper(I) in Ionic Liquid-reline,” *Chemical Research in Chinese Universities* **29** (2013), pp. 991-997.

[44] Ana-Maria Popescu, Virgil Constantin, Anca Cojocaru, Mircea Olteanu, “Electrochemical Behaviour of Copper (II) Chloride in Choline Chloride-urea Deep Eutectic Solvent,” *Rev. Chim. (Bucharest)* **62** (2011), pp. 206-213.

[45] M. Rostom Ali, Md. Ziaur Rahman, S. SankarSaha, “Electrodeposition of Copper from a Choline Chloride based Ionic Liquid,” *Journal of Electrochemistry* **20** (2014), pp. 139-145.

[46] Qingwei Chua, Jun Lianga, Jingcheng Haoa, “Electrodeposition of zinc-cobalt alloys from choline chloride–ureaionic liquid,” *Electrochimica Acta* **115** (2014), pp. 499–503.

[47] Andrew P. Abbott, Glen Capper, Katy J. McKenzie, Karl S. Ryder, “Electrodeposition of zinc–tin alloys from deep eutectic solvents based on choline chloride,” *Journal of Electroanalytical Chemistry* **599** (2007), pp. 288–294.

[48] E. Gómez, E. Vallés, “Platinum Electrodeposition in an Ionic Liquid Analogue. Solvent Stability Monitoring,” *Int. J. Electrochem. Sci.* **8** (2013), pp.1443 - 1458.

[49] S. Costovici, A. Petica, C-S Dumitru, A. Cojocaru, L. Anicaia, “Electrochemical Synthesis of ZnO Nanopowder Involving Choline Chloride Based Ionic Liquids,” *Chemical Engineering Transactions* **41** (2014), pp. 343-348.

[50] L. Anicai, A. Florea, T. Visan, “Studies Regarding the Nickel Electrodeposition from Choline Chloride Based Ionic Liquids,” *Applications of Ionic Liquids in Science and Technology*, Middle Tennessee State University, USA, September 2011, pp. 261-286.

[51] T-C Huynh, Quang P. D. Dao, T-N Truong, N-G Doan, Son-Lam Ho, “Electrodeposition of Aluminum on Cathodes in Ionic Liquid Based Choline Chloride/Urea/ AlCl_3 ,” *Environment and Pollution* **3** (2014), pp. 59-69.

[52] F. Golgovici, T. Visan, “Electrodeposition behavior of cadmium telluride from chlorine chloride-urea ionic liquids,” *Chalcogenide Letters* **9** (2012), pp. 165-174.

- [53] Min Li, Zhaowen Wang, Ramana G. Reddy, "Cobalt electrodeposition using urea and choline chloride," *Electrochimica Acta* **123** (2014), pp. 325–331.
- [54] A. J. Bard, L. R. Faulkner, *Electrochemical Methods: Fundamental and Applications*. New York, John Wiley & Sons (1980).
- [55] D. Pradhan, Ph.D Dissertation, the University of Alabama (2010), pp. 1-178
- [56] D. Pradhan, R. G. Reddy, D. Mantha, "Dendrite Free Aluminum Electrodeposition using Ionic Liquid Electrolyte," *Proceedings of the Sadoway 60 Symposium*, MIT, Cambridge, Massachusetts, USA (2010), pp. 106-112.
- [57] R. G. Reddy, "Low Temperature production of zinc from zinc oxide," *Carbon Management Technology Conference, CMTC*, Orlando, FL (2012), pp. 1-6.
- [58] D. Pradhan, R. G. Reddy, "Low Temperature Electrochemical Synthesis of Ti-Al Alloys using Ionic Liquid Electrolytes," *TMS*, Warrendale, USA (2008), pp. 345-352.
- [59] D. Pradhan, R. G. Reddy, "Effect of electrode physical properties on dendritic deposition of aluminum using EmimCl-AlCl₃ ionic liquid electrolyte," *TMS Warrendale, USA* (2009), pp. 17-24.
- [60] D. Yue, Y. Jia, Y. Yao, Y. Sun, Y. Jing, "Structure and electrochemical behavior of ionic liquid analogue based on choline chloride and urea," *Electrochim. Acta* **65** (2012), pp. 30–36.
- [61] Q.Q. Yang, K.R. Qiu, D.R. Zhu, L.C. Sa, "Electrodeposition of cobalt and rare earthcobalt in urea-NaBr-KBr melt," *Electrochemistry* **1** (1995), pp. 274-277.
- [62] C.W. Xu, W.J. Pan, D.S. Yuan, Y.X. Tong, G.K. Liu, "Preparation of Gd-Co alloy film in acetamide-urea-NaBr melt," *T. Nonferr. Metal. Soc.* **12** (2002), pp. 1007-1010.
- [63] J.C. Wang, C.W. Xu, P. Liu, Y.X. Tong, G.K. Liu, "Preparation of Y-Co alloy film in acetamide-urea-NaBr melt," *T. Nonferr. Metal. Soc.* **12** (2002), pp. 1191-1194.
- [64] C.N. Su, M.Z. An, P.X. Yang, H.W. Gu, X.H. Guo, "Electrochemical behavior of cobalt from 1-butyl-3-methylimidazolium tetrafluoroborate ionic liquid," *Appl. Surf. Sci.* **256** (2010), pp. 4888–4893.
- [65] Li M, Wang ZW, Reddy RG, "Electrodeposition of cobalt from air and water-stable ionic liquid 1-butyl-3- methylimidazolium tetrafluoroborate," In: Yurko J, Zhang LF, Allanore A, Wang C, Spangenberg JS, Kirchain RE, Downey JP, May LD (eds) *aterials processing fundamentals. EPD Congress, San Diego*, (2014), pp. 241–250.
- [66] Fukui R, Katayama Y, Miura T, "The effect of organic additives in electrodeposition of Co from an amide-type ionic liquid," *Electrochim Acta* **56** (2011), pp. 1190–1196.

[67] Carlin RT, De Long HC, Fuller J, Trulove PC, "Microelectrode evaluation of transition metal-aluminum alloy electrodepositions in chloroaluminate ionic liquids," J Electrochem Soc. **145** (1998), pp. 1598–1607.

[68] D. Pradhan, R.G. Reddy: "Mechanistic study of Al electrodeposition from EMIC-AlCl₃ and BMIC-AlCl₃ electrolytes at low temperature," Mater. Chem. Phys. **143** (2013), pp. 564-569.

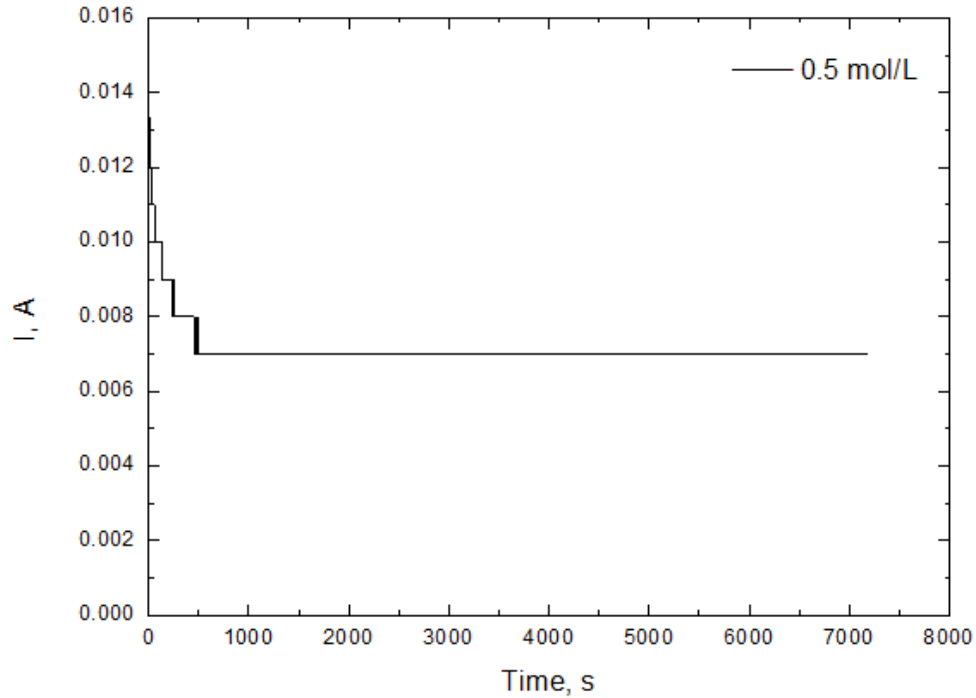
[69] Q. Liao, W. R. Pitner, G. Stewart, C. L. Hussey, G. R. Stafford, "Electrodeposition of Aluminum from the Aluminum Chloride-1-Methyl-3-ethylimidazolium Chloride Room Temperature Molten Salt + Benzene," J. Electrochem. Soc. **144** (1997), pp. 936-943.

APPENDIX I

CALCULATION OF CURRENT EFFICIENCY AND ENERGY CONSUMPTION

FROM COBALT ELECTRODEPOSITION

From the experiment performed with the copper cathode, the graphite anode with concentration 0.5 M of CoCl_2 , the applied voltage 2.7V at 323K for 2 hours



The current efficiency (η) of the electrodeposition can be calculated by following equation:

$$\eta = \frac{m_1}{m_2} \times 100\% \quad (\text{I-1})$$

where m_1 is the weight of the deposited cobalt on the cathode in gram, its value can be calculated from the weight difference of the cathode before and after the electrodeposition. m_2 is the theoretical weight of cobalt in gram which is already used to calculate the additional Co during the experiment. m_2 , the theoretical weight of cobalt in grams, can be calculated using Faraday's law [23]:

$$m_2 = \frac{Ita}{nF} \quad (\text{I-2})$$

where I is the applied current in A, t is the deposition time in s, a is the molecular weight of cobalt, and F is Faraday constant.

Using the equations above, the weight of deposited cobalt on cathode is

$$m_1 = 2.8649 - 2.85 = 0.0149 \text{ (g)}$$

The theoretical weight of cobalt is

It = the area under the curve = 51.3686 A·s;

$$m_2 = \frac{51.3686 \times 58.93}{2 \times 96500} = 0.0158 \text{ (g)}$$

Thus, the current efficiency (η) is :

$$\eta = \frac{0.0149}{0.0158} \times 100\% = 94.9969 \%$$

The energy of consumption (E) is the measure of consumption of power and can be calculated by:

$$E = V \frac{Q}{\eta} \quad (\text{I-3})$$

where V is the reduction voltage used in this experiment, Q is the total charge required for the certain amount deposit of cobalt on cathode, and η is the current efficiency on the cathode.

Applying the experiment data to the equation (I-3),

V = applied voltage = 2.7 V

η = 94.9969 %

$Q = i \cdot t$ = area under the curve = 51.3686 A·s = 51.3686 (Coulomb)

0.0158 g of Co deposit (theoretical) requires = 51.3686 (Coulomb)

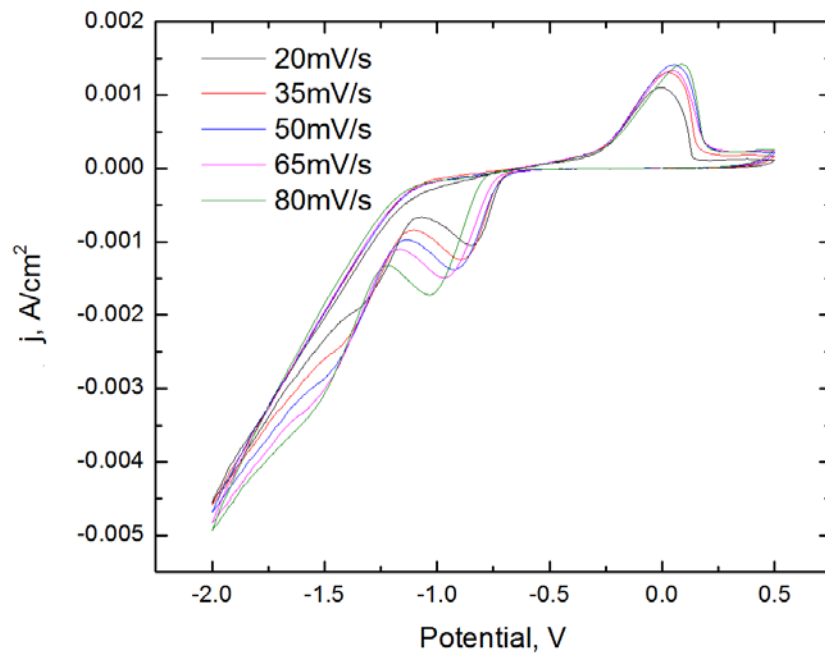
$$\text{Charge /1000g} = \frac{51.3686 \times 1000}{0.01568} = 3276052 \text{ (Coulomb)}$$

$$\text{Energy Consumption (E)} = \frac{2.7 \times 3276052 \times 100}{94.9969 \times 1000 \times 3600} = 2.5847 \text{ (kWh/kg of Co)}$$

APPENDIX II

CALCULATION OF THE TRANSFER COEFFICIENT AND THE DIFFUSION COEFFICIENT FROM CYCLIC VOLTAMMETRY CURVE

From the cyclic voltammetry curve



Scan Rate (mV/s)	Cathodic Peak Potential (V)	Half Cathodic Potential (V)
20	-0.8515	-0.7625
35	-0.891	-0.7872
50	-0.9257	-0.797
65	-0.9652	-0.8267
80	-1.0347	-0.891

The equation to calculate the transfer coefficient is:

$$|E_p - E_{p/2}| = 1.857RT/\alpha nF \quad (\text{II-1})$$

$$\alpha = \frac{1.857RT}{nF|E_p - E_{p/2}|} \quad (\text{II-2})$$

where E_p is the cathodic potential in V, $E_{p/2}$ is the half of the cathodic potential in V, R is the gas constant which is, T is the temperature in K, α is the transfer coefficient, n is the number of exchanging electrons, and F is the Faraday constant, 96500 C/mol.

For the scan rate 20mV/s,

$$|E_p - E_{p/2}| = |-0.8515 - (-0.7625)| = 0.089 \text{ (V)}$$

$$R = \text{Gas constant} = 8.314 \text{ J/K*mol}$$

$$T = \text{Experimental temperature in K} = 323 \text{ K}$$

$$n = \text{number of electrons} = 2$$

$$F = \text{Faraday constant} = 96500 \text{ C/mol}$$

$$\alpha = \frac{1.857 \times 8.314 \times 323}{2 \times 96500 \times 0.089} = 0.2903$$

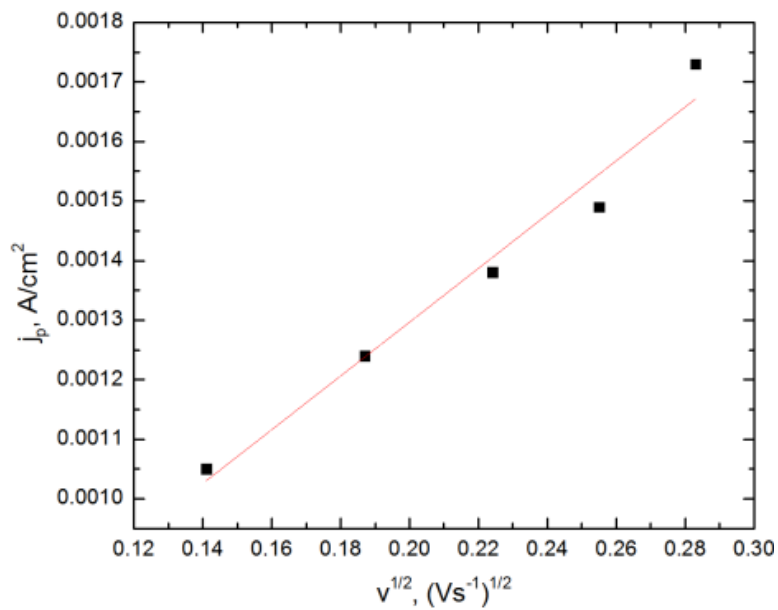
Using this calculation for each scan rate, the average transfer coefficient is:

$$\alpha_{\text{ave}} = \frac{0.29+0.25+0.2+0.19+0.18}{5} = 0.22$$

Following equation is to calculate the diffusion coefficient of cobalt ion in electrolyte at 323K:

$$I_p = 0.4958nFAc^i \left(\frac{\alpha nF}{RT}\right)^{1/2} D^{1/2} \nu^{1/2} \quad (\text{II-3})$$

where I_p is the cathodic peak current in A, A the electrode area in cm^2 , c^i is the initial concentration in mol/cm^3 , α is the coefficient transfer, D is the diffusion coefficient in cm^2/s , and ν is the scan rate in V/s .



Scan Rate (mV/s)	Cathodic Potential Peak (V)	Cathodic Peak Potential (A)
20	-0.8515	-0.00105
35	-0.891	-0.00124
50	-0.9257	-0.00138
65	-0.9652	-0.00149
80	-1.0347	-0.00173

From the linear plot of the cathodic potential as a function of scan rates (Figure 5.3),

$$y = 0.0045x + 0.0004$$

Using the relationship between the slope and the equation,

$$0.4958nFAc^i\left(\frac{\alpha nF}{RT}\right)^{1/2}D^{1/2} = 0.0045$$

$$A = \text{tungsten electrode area} = 0.0025^2 \times \pi + 0.005 \times 1 \times \pi = 0.0157(\text{cm}^2)$$

$$T = 323 \text{ K}$$

$$c^i = 0.2 \text{ M}$$

The diffusion coefficient can be calculated by substituting variables:

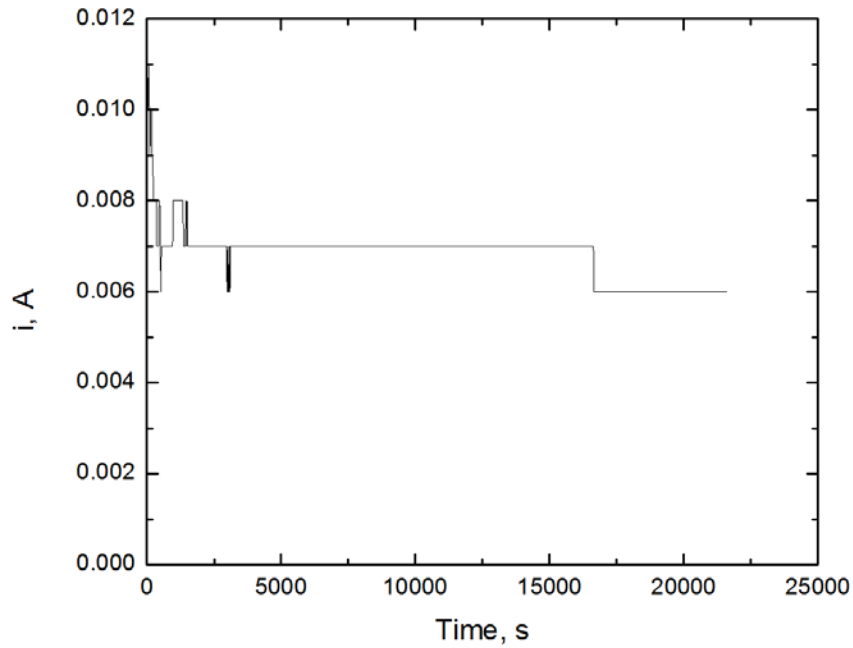
$$0.4958 \times 2 \times 96500 \times 0.0157 \times 0.2 \times \left(\frac{0.22 \times 2 \times 96500}{8.314 \times 323}\right)^{1/2} \times D^{1/2} = 0.0045$$

$$D = 3.3766 \times 10^{-6} \text{ cm}^2/\text{s}$$

APPENDIX III

RESULT OF COBALT DEPOSITS ON COPPER ELECTRODE FOR 6 HOUR

EXPERIMENT



Parameters	Co on copper cathode
Working Electrode	Cu (2cm × 2.5cm)
Counter Electrode	C (2cm × 2.5cm)
Concentration of CoCl ₂	0.5 M
Temperature	323K
Applied Voltage	2.7 V
Time	6 hours
Electrodes Distance	2 cm

$$Q = \text{Area under the curve} = 147.3014 \text{ A} \cdot \text{s}$$

$$m_1 = 2.923 - 2.881 = 0.042 \text{ (g)}$$

$$m_2 = \frac{147.3014 \times 58.93}{2 \times 96500} = 0.0450 \text{ (g)}$$

Thus, the current efficiency (η) is

$$\eta = \frac{0.042}{0.0450} \times 100\% = 93.3820 \%$$

After the calculation of the energy consumption as Appendix I,

Concentration of CoCl ₂ (mol/L)	Temperature (K)	Cell Voltage (V)	η (%)	E (kWh/kg)
0.5	323	2.7	93.38	2.63

Since a bit amount of cobalt deposits were lost during collecting from a magnetic stirrer, the current efficiency is less than that of the result from 2 hour experiment data with the same parameters. Considering that fact, this parameter is able to produce the high purity cobalt deposits with the lower energy consumption regardless the experiment conducting time.